SOUTHERN CALIFORNIA PARTICLE SUPERSITE

Progress Report for Period December 1, 2002 – March 31, 2003

United States Environmental Protection Agency

Principal Investigator: John R. Froines, Ph.D., UCLA School of Public Health

Co-Principal Investigator: Constantinos Sioutas, Sc.D., USC School of Engineering

1. Introduction

The overall objective of the Southern California Particle Supersite is to conduct research and monitoring that contributes to a better understanding of the measurement, sources, size distribution, chemical composition and physical state, spatial and temporal variability, and health effects of suspended particulate matter (PM) in the Los Angeles Basin (LAB). This report addresses the period from December 1, 2002 to March 31, 2003. It is divided into 15 sections, each addressing a specific research area. Furthermore, a major portion of the information included in this report has been either submitted or accepted for publication in peer-reviewed journals. Below is a list of manuscripts either submitted or accepted for publication which were produced through the Southern California Supersite funds and in which the EPA Supersite program has been acknowledged.

2. Publications

The Southern California Particle Supersite has been acknowledged so far in the following publications:

1. Misra, C., Geller, M., Sioutas, C and Solomon P. "Development and evaluation of a continuous coarse particle monitor". *Journal of Air and Waste Management Association*, 51:1309-1317, 2001

2. Geller, M.D., Kim, S. Misra, C., Sioutas, C., Olson, B.A and Marple, V.A. "Methodology for measuring size-dependent chemical composition of ultrafine particles " *Aerosol Science and Technology*, 36(6): 748-763, 2002

3. Misra, C., Kim S., Shen S. and Sioutas C. "Design and evaluation of a high-flow rate, very low pressure drop impactor for separation and collection of fine from ultrafine particles". *Journal of Aerosol Science*, 33(5): 735-752, 2002

4. Li, N., Kim, S., Wang, M., Froines, J.R., Sioutas, C. and Nel, A. "Use of a Stratified Oxidative Stress Model to Study the Biological Effects of Ambient Concentrated and Diesel Exhaust Particulate Matter". *Inhalation Toxicology*, 14(5): 459-486, 2002

5. Zhu, Y., Hinds, W.C., Kim, S and Sioutas, C. "Concentration and Size Distribution of Ultrafine Particles near a Major Highway". *Journal of Air and Waste Management Association*, 52:1032-1042, 2002

6. Singh, M., Jaques, P. and Sioutas, C. "Particle-bound metals in source and receptor sites of the Los Angeles Basin". *Atmospheric Environment*, 36(10): 1675-168, 2002

7. Kim, S., Shi, S., Zhu, Y., Hinds, W.C., and Sioutas, C. "Size Distribution, Diurnal and Seasonal Trends of Ultrafine Particles in Source and Receptor Sites of the Los Angeles Basin". *Journal of Air and Waste Management Association*, 52:174-185, 2002

8. Misra, C., Singh, M., Hall, P. and Sioutas, C. "Development and evaluation of a personal cascade impactor sampler (PCIS)". *Journal of Aerosol Science*, 33(7), 1027-1047, 2002

9. Eiguren-Fernandez A., Miguel A.H, Jaques, P. and Sioutas, C. "Evaluation of a Denuder-MOUDI-PUF Sampling System to Determine the Size Distribution of Semivolatile Polycyclic Aromatic Hydrocarbons in the Atmosphere". *Aerosol Science and* Technology, 37: 201-209, 2003

10. Fine, P.M., Hering, S.V., Jaques P.A. and Sioutas, C. "Performance Evaluation and Field Use of a Continuous Monitor for Measuring Size-Segregated PM2.5 Particulate Nitrate". *Aerosol Science and Technology*, 37: 342-354, 2003

11. Singh, M., Misra, C., and Sioutas, C. "Field Evaluation of a Particle Monitor for Size-Dependent Measurement of Mass and Chemical Composition of Individual Exposures to PM". Manuscript submitted to *Aerosol Science and Technology*, June 2002.

12. Shen, S., Zhu, Y., Jaques PA and Sioutas C. "Evaluation of the SMPS-APS system as a Continuous Monitor for PM2.5 and PM10". *Atmospheric Environment*, 36, 3939-3950, 2002

13. Zhu, Y., Hinds, W.C., Kim, S., Shen, S. and Sioutas, C. "Study on Ultrafine Particles and other Vehicular Pollutants near a Busy Highway". *Atmospheric Environment*. 36, 4375-4383, 2002

14. Misra, C., Geller, M.D., Solomon, P.A. and Sioutas, C. "Development of a PM10 Inertial Impactor for Coarse Particle Measurement and Speciation." *Aerosol Science and Technology*, 37:271-282, 2003

15. Zhu, Y., Hinds, W.C., Kim, S., Shen, S. and Sioutas, C. "Seasonal Trends of Concentration and Size Distributions of Ultrafine Particles Near Major Freeways in Los Angeles". *Aerosol Science and Technology*, in press, April 2003

16. Misra, C., Geller, M., Fine, P.M.. and Sioutas, C. "Development and Evaluation of an Ultrafine Particle Concentrator Facility for Human Exposures". Submitted to *Aerosol Science and Technology*, September 2002.

17. Gong, H.Jr, Linn, W.S., Sioutas, C., Terrell S.L., Clark, K.W., Anderson K.R and Terrell, L . "Controlled Exposures of Healthy and Asthmatic Volunteers to Concentrated Ambient Fine Particles in Los Angeles". *Inhalation Toxicology*, 15(4), 305-325.

18. Li, N., Sioutas, C , Froines, J.R., Cho, A., Misra, C and Nel, A., "Ultrafine Particulate Pollutants Induce Oxidative Stress and Mitochondrial Damage" *Environmental Health Perspectives*, in press, December 2002

19. Chakrabarti, B., Singh, M and Sioutas C. "Development of a Continuous Monitor For Measuring the Mass Concentration of Ultrafine PM." *Aerosol Science and Technology*, in press, January 2003

20. Jaques, P.A., Ambs, J.L. and Sioutas, C. "Field Evaluation Of The Differential TEOM® Monitor For Continuous PM2.5 Mass Concentrations ". Submitted to *Aerosol Science and Technology*, September 2002

21. Zhu, Y., Hinds, W.C. and Sioutas, C. "Vertical Profile of Ultrafine Particles in the Vicinity of a Major Highway". Submitted to *Atmospheric Environment*, December 2002

22. Fine, P.M., Si, S., Geller, M.G., and Sioutas, C. "Diurnal and Seasonal Characteristics and Size of Ultrafine PM in Receptor Areas of the Los Angeles Basin". *Aerosol Science and Technology*, in press, 2003

23. Chakrabarti, B., Fine, P.M, Delfino R.J. and Sioutas C. "Performance Evaluation of an active personal DataRAM PM2.5 mass monitor (Thermo Anderson pDR-1200) designed for continuous personal exposure measurements" Submitted to *Atmospheric Environment*, February 2003

24. Yu, R.C., Teh, H.W., Sioutas, C. and Froines, J.R. "Quality Control of Semi-Continuous Mobility Size-Fractionated Particle Number Concentration Data". Submitted to *Atmospheric Environment*, February 2003

25. Miguel, A.H., Eiguren-Fernandez, A., Jaques, P.A., Mayo, P.R. and Sioutas, C. "Seasonal variation of the particle size distribution of polycyclic aromatic hydrocarbons and of major aerosol species in Claremont, California" Submitted to *Atmospheric Environment*, February 2003

3. PIU Sampling Location and Status

A key feature of our Supersite activities has been in the ability to conduct state-of the art measurements of the physiochemical characteristics of PM in different locations of the Los Angeles basin (LAB). We originally proposed a 2.5-year repeating cycle of measurements at five locations. Each location has been scheduled to sample during a period of intense photo-chemistry (defined approximately as May-October) and low photochemical activity (defined as the period between November-April). During the period of this progress report, we've continued PM

sampling with the Particle Instrumentation Unit (PIU) at the University of Southern California (USC), the fifth Southern California Supersite location, beginning September 2002. The site is located about one mile directly south of downtown Los Angeles and the 10 Freeway, which runs east to west, and is about 100 meters directly east of the 110 Freeway. The site is embellished with typical urban sources: centralized within a major congested urban center; adjacent to several 2 – 7 story buildings; adjacent to pedestrian and local traffic as well as central arteries; and near building and road construction projects. Since the site is about 15 miles directly east-north-east of the ocean, prevailing winds are primarily from the west and south-west during most of the daytime when mobile and stationary emission sources may be expected to predominate. However, the nearby relatively large buildings can also disturb the winds, affecting urban canyon and wake properties. These factors consist of turbulent winds and updrafts that may confound local measurements of regional wind trajectories, and increase the delivery of local sources (e.g., construction debris, and larger settled particles from road related vehicle wear-and-tear) in addition to the close-by 110 Freeway. Several studies are being conducted as we enter the 3rd quarter at the USC site to investigate local source contributions in addition to the regional transported emissions that may generally come from the west freeways.

We have completed all Metal/Element speciation analysis for integrated samples, through most of February, and Ion and EC/OC speciation analysis through early January. Also, we have continued to make size integrated on-line measurements of particulate nitrate and carbon using the Integrated Collection and Vaporization System (ICVS) developed by Aerosol Dynamics Inc. Semi-continuous PM2.5 measurements continue to be made with a set of prototype Differential TEOMs, designed to measure "non-artifact" laden mass. Two continuous BAM monitors have been operating: one, with the standard PM2.5 inlet, the second with an ultrafine concentrator inlet (designed at our USC lab). Coupled with our USC-TEOM coarse monitor, time-integrated mass measurements are being compared to those by our SMPS-APS and Differential ESP TEOM for short term periods, and to MOUDI, Partisol, and other filter mass samplers for longer sample integrals, overall, resulting in paired integrated semi-continuous, diurnal, and 24-hour mass measurements of coarse, fine, and ultrafine PM.

Additionally, we have continued to make our mobile particle trailer available for co-located exposure studies. The following health studies have been supported by the Supersite measurements: In vitro studies undertaken by Drs. Andre Nel and Arthur Cho (UCLA) investigating the hypotheses that organic constituents associated with PM, including quinines, other organic compounds (PAHs, nitro-PAHs, and aldehydes/ketones) and metals are capable of generating reactive oxygen species (ROS) and acting as electrophillic agents. These are ongoing studies. Animal inhalation toxicology studies using Concentrated Ambient Particulates (CAP) investigating the hypotheses that atmospheric chemistry is important in the toxicity of PM and co-pollutants, airway injury and cardiovascular effects will be greater at receptor sites downwind of source sites along the mobile source trajectory in the Los Angeles basin. Led by Drs. Harkema (University of Michigan), Kleinman (UC Irvine), Froines, and Nel (UCLA), these co-located studies have commenced during our first month at the USC site. Additionally, as with Claremont, exposure studies will continue throughout this winter to investigate seasonal changes in toxicity near this urban site.

4. Time Integrated Size Fractioned Chemical Speciation for USC

Introduction

This section, on integrated sampling, exclusively reports our recent progress at the USC location, between commencements of sampling (early October 2002) through this past mid-winter. Section 5 is more comprehensive, and reports a full summary of time-integrated mass and chemically speciated results for the full 3 years that the PIU has been monitoring in the LA Basin.

Our current sampling scheme continues to involve the use of three MOUDI's for 24-hour averages: size-fractionated measurements of ambient and concentrated PM mass and chemical composition. Additionally, a Partisol is used to acquire the coarse fraction of mass. Sampling is conducted once a week, typically on Tuesday, Wednesday or Thursday. However, this schedule is flexible to be adjusted for our "intensive" particulate characterization studies and/or for our support of co-located health effects exposure studies. Typically, ambient data are averaged over 24 hours (midnight to midnight), whereas for exposure or source contribution measurements, the time integrals may vary. Except for special studies that may involve other size cuts, consistent with our original Supersite proposal, we have used three collocated Micro-Orifice Uniform Deposit Impactors (MOUDI) to generate five PM size ranges:

<0.1 μm	(ultrafine particles)
0.1- 0.32 μm	(accumulation mode, "condensation" sub-mode)
0.32 – 1.0 μm	(accumulation mode, "droplet" sub-mode)
1.0 – 2.5	("intermediate" mode)
2.5-10 μm	(coarse particles)

In addition to mass concentration, the following chemical components have been analyzed within these size groups: inorganic ions (i.e., sulfate, nitrate, ammonium), analyzed by ion chromatography (Dionex); trace elements and metals, analyzed by XRF; and the elemental and organic carbon (EC/OC) content is analyzed by thermal optical detection. For USC, sample analysis has been completed to between early January through middle February for chemical and mass data. Mass and chemical size fractionated data are presented for the USC site, below.

Results

For the USC site, most of the size fractionated chemical and mass integrated results are similar to those of the last report, except for a few observed changes, as noted below. Overall, the results may suggest that, on a 24-hour basis, patterns were based on local urban sources, which would be expected at this site.

Figure 1 presents 24 hour averaged size segregated mass. The results show that, on the average, the coarse and fine fractions are about equivalent to each other, between about 21 and 23-ug/m3. Also, the PM2.5 cumulative mass of the MOUDI stages is nearly identical to that of the Partisol, exemplifying the relatively high level of reliability for both. The "droplet" sub-mode predominates at about 8 ug/m3, nearly twice as great as the adjacent modes, and about 3 ug/m3 less than in the previous report. The site is about 100 meters downwind of the 110 freeway On-

Ramp. It is expected to receive freshly generated mobile source PM (e.g., Zhu, et al., 2002), but may be confounded by local coarse particles that could come from vehicle-to-road wear-and-tear, as well as local construction debris, all re-suspended via the urban canyon wake effect that is present at this site.

Figure 2 presents size segregated 24hour NH4NO3 and (NH4)2SO4, while Figure 3 presents that for EC and OC. PM 2.5 mass predominates for all chemical groups. The droplet mode for NO3, SO4, and OC dominates in the Fine fraction, while the nuclei (<0.1 um) and condensation modes do for EC, which suggests local mobile source emissions. However, the local construction may add to this mass when using combustion related equipment. Generally, this speciated data corresponds with the mass measurements. On a relative basis (see Figure 3b), OC accounts for more than 80% of the Total Carbon (as measured using the NIOSH-based Thermal Desorption analytical technique) for all sizes, including the nuclei and accumulation modes.

Figures 4 and 5 present size segregated mass and relative-mass for Anthropogenic and Crustal speciated source metal elements, respectively. In contrast to the "Crustal" source metals, the "Anthropogenic" source metals are much higher for PM2.5, which is nearly equivalent to the coarse fraction for this group of elements. In addition, the Crustal metal elements clearly predominate by between 60 and 80% in the coarse mode, and account for about 10% of the intermediate mode.

Especially noteworthy, and in contrast to the previous report, is the unusually high Al in the nuclei and condensation modes. This is likely not due to sampling artifacts, as the concentrations are unique to Al, and in contrast to the other Crustal-source metals that are typically associated, by size and source, with Al. The likely source of the measured primary Al-associated particles may be from fumes generated by welding at the construction site that is located about 100 meters directly south-south-west of the PIU.

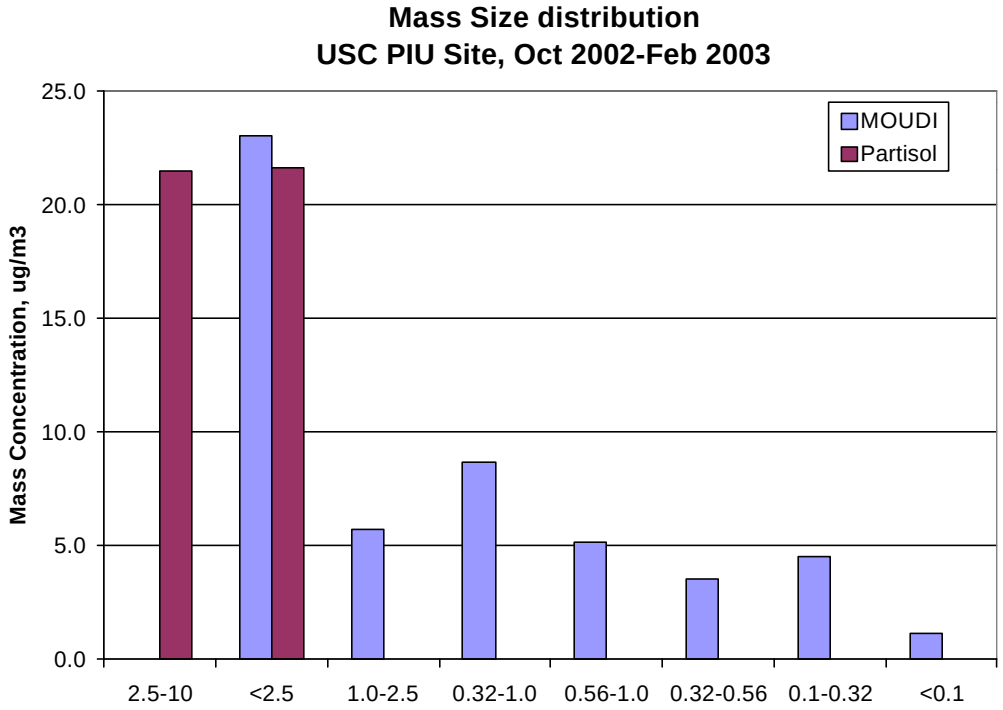

Figure 1. MOUDI and Partisol size fractionated measurements of ammonium nitrate and Sulfate at USC PIU site for October 2002, 2002 through February, 2003.

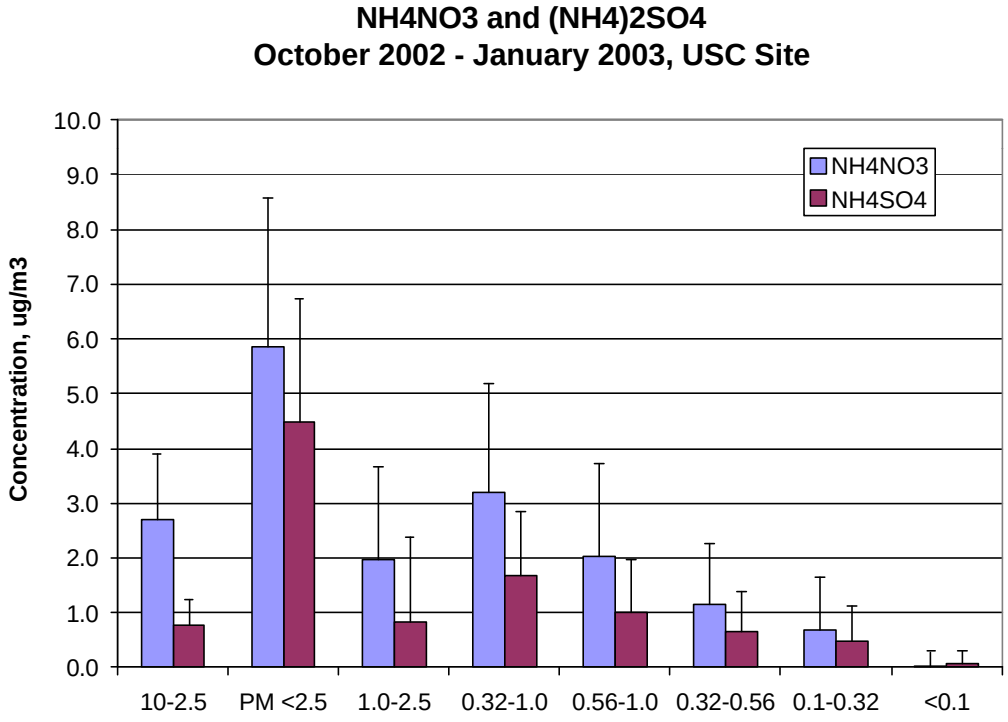

Figure 2. MOUDI size fractionated measurements of ammonium nitrate and Sulfate at USC PIU site for October, 2002 through January, 2003.

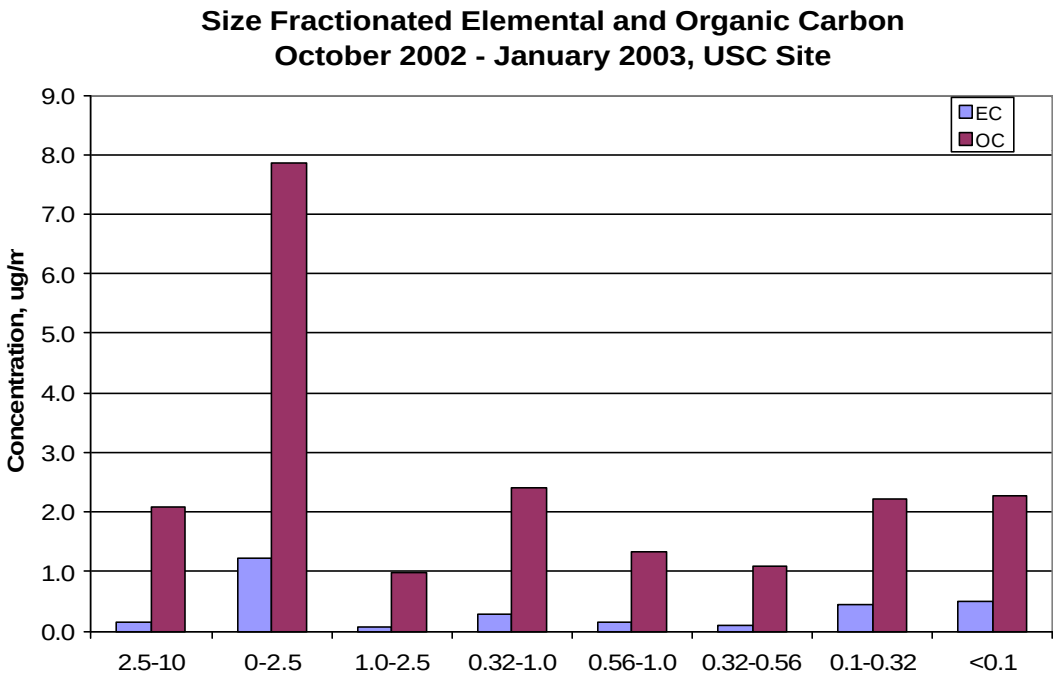

Figure 3a. MOUDI size fractionated measurements of Elemental and Organic Carbon at USC PIU site for October, 2002 through January, 2003.

Figure 3b. Relative (N=7) MOUDI size fractionated measurements of Elemental and Organic Carbon at USC PIU site for October, 2002 through January, 2003.

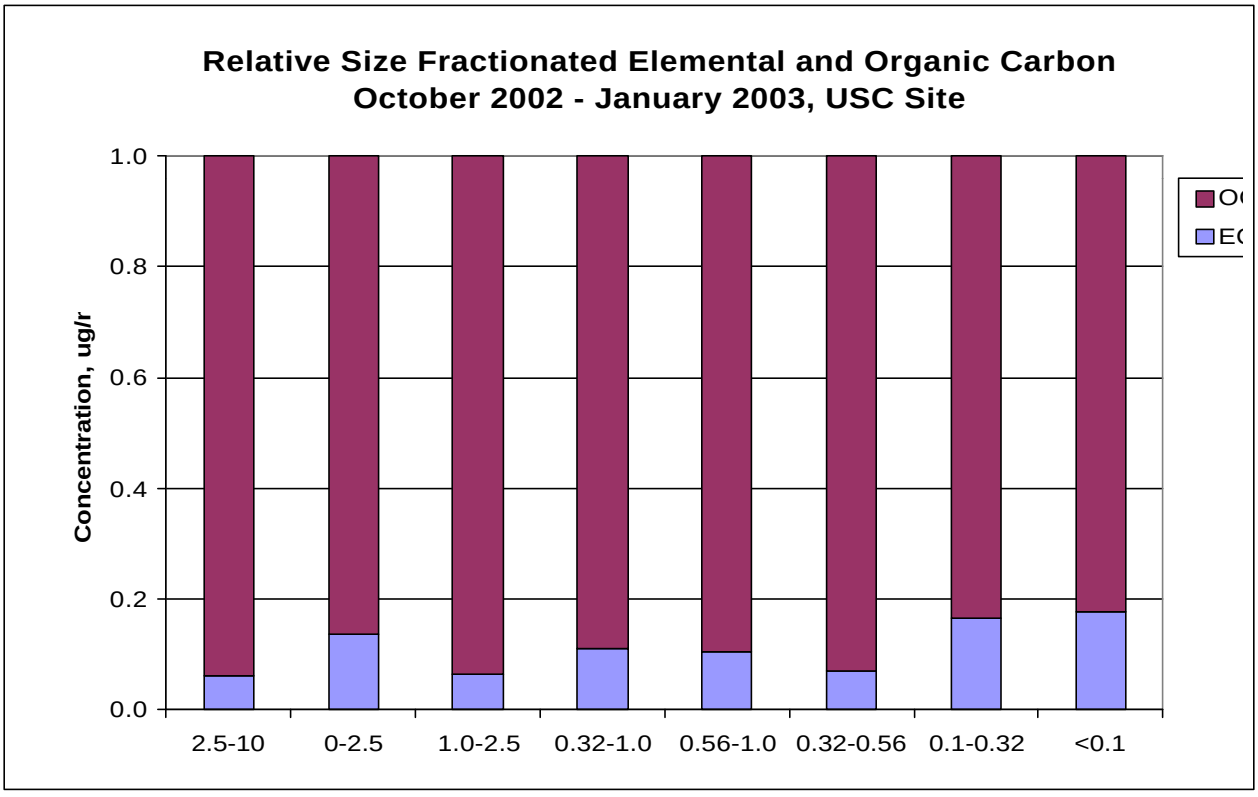

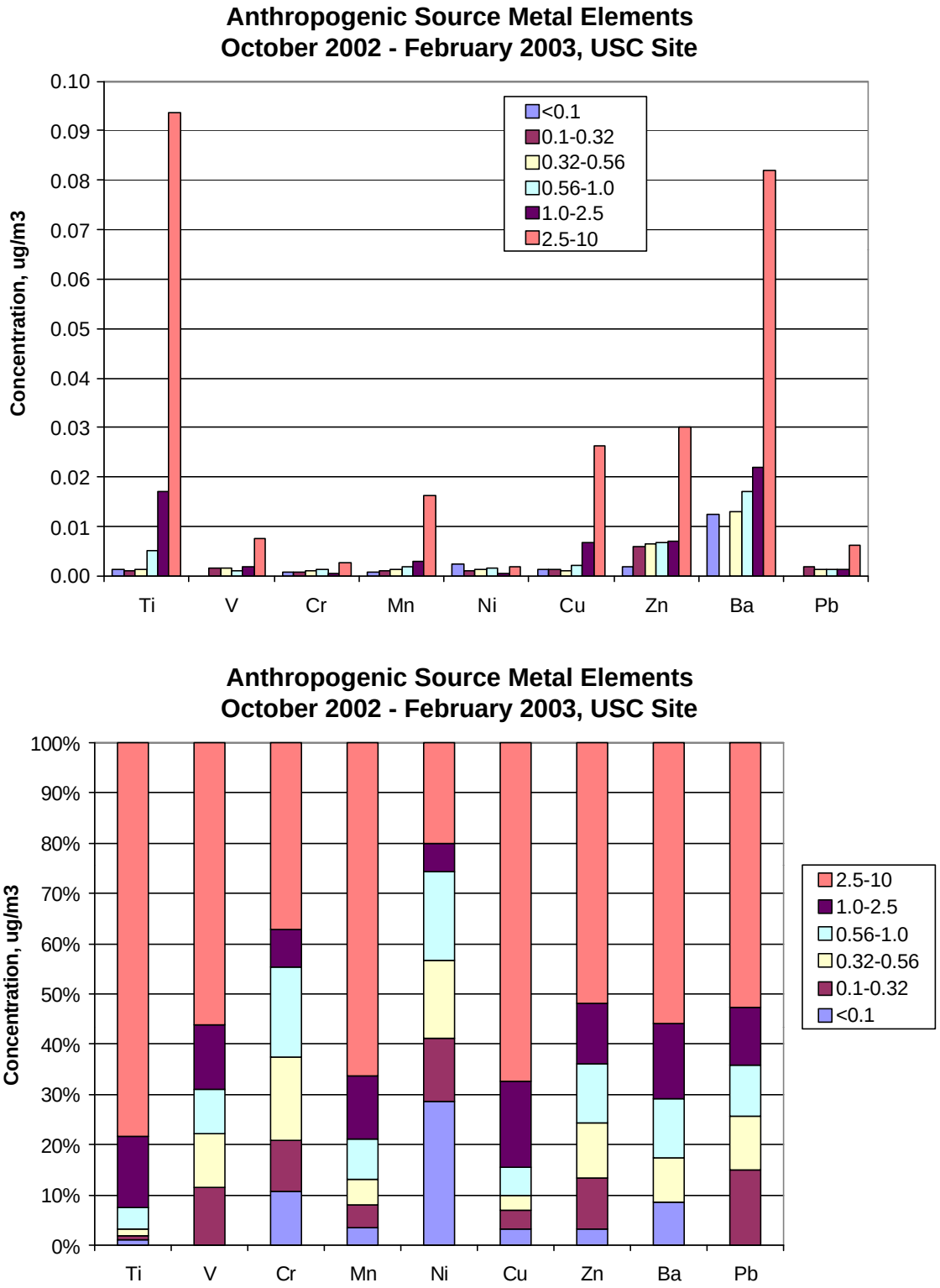

Figure 4. a) Concentration & b) Relative Concentration of Metal Elements typically found in anthropogenic sources.

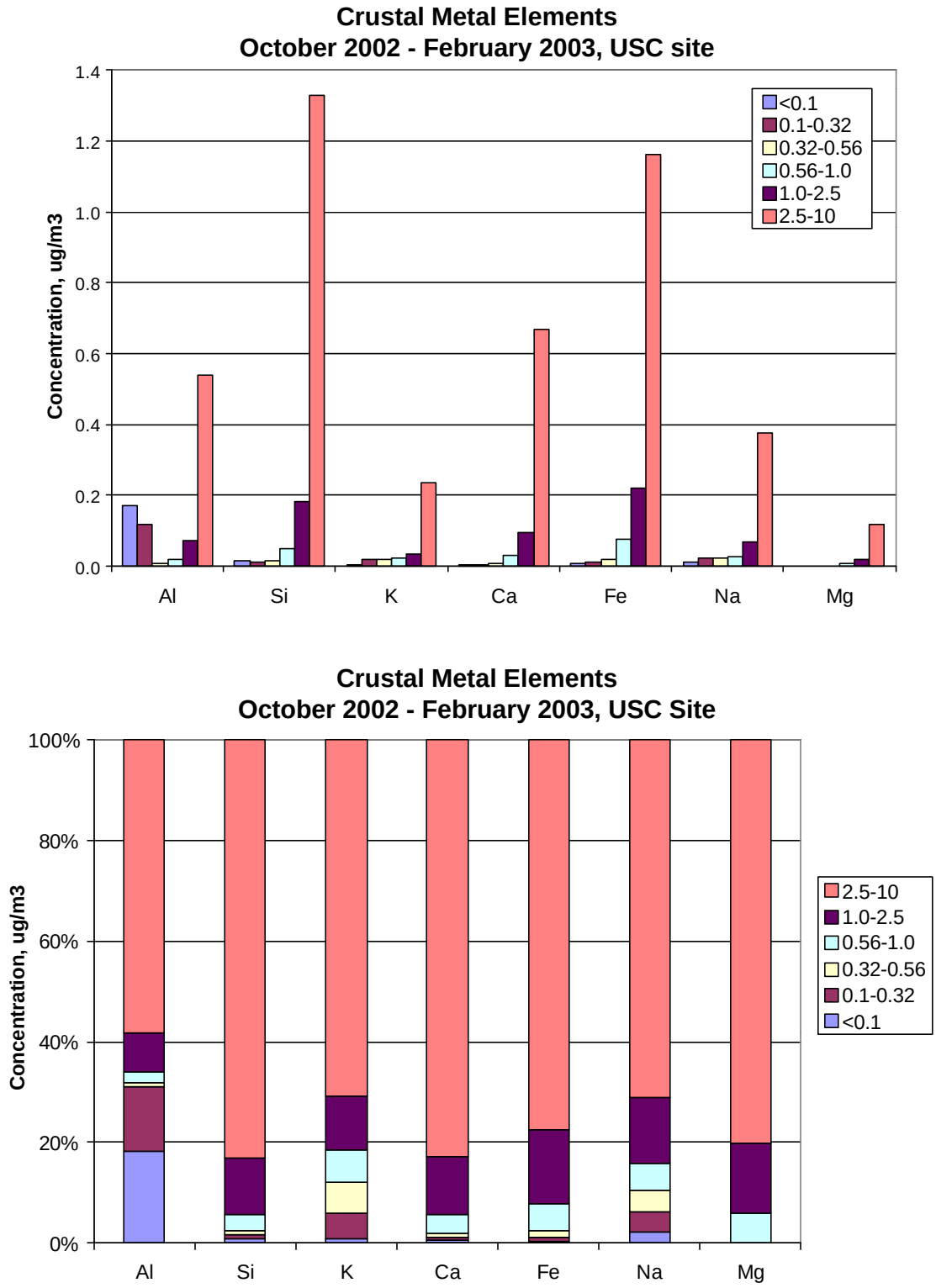

Figure 5. a) Concentration & b) Relative Concentration of Metal Elements typically found in crustal sources.

5. Time integrated, size fractionated mass and chemical speciation for five sites in the Los Angeles Basin.

Introduction:

Sampling was conducted at five locations in the Los Angeles Basin over a period of more than two years. The sites and the period of sampling is given in Table 1. Three MOUDI samplers were deployed and collected 24-hour samples for size-fractionated ambient PM mass and chemical composition. The MOUDI samples were analyzed for sulfate, nitrate, EC, OC and individual metals. The PM size ranges measured are <0.1 μm (ultrafine), 0.1- 0.32 μm, 0.32 – 1.0 μm and 1.0 – 2.5, (these three sizes comprising the accumulation mode) and 2.5-10 μm (coarse mode). A Partisol sampler was also used to in some cases to measure coarse PM properties. The inorganic ions, sulfate and nitrate are analyzed by ion chromatography (Dionex), trace elements and metals by XRF and the elemental and organic carbon (EC and OC) by thermal evolution/optical transmission analysis.

Table 1

Site	**Period of Sampling**
Downey	**Oct 2000 – Feb 2001**
Riverside	**Feb 2001 – June 2001**
Rubidoux	**June 2001 – Sept 2001**
Claremont	**Sept 2001 – Aug 2002**
USC	**Oct 2001 – Ongoing**

Results and discussion:
Figure1 shows the monthly average mass distribution in the three modes (coarse, accumulation and ultrafine) for all five sites. The highest ultrafine concentration were observed in Downey. The accumulation mode concentration increases in summer and decreases in winter across all sites, but especially at the receptor sites (Riverside, Rubidoux and Claremont). This trend may be due to increased advection with higher wind speeds in the summer. Furthermore, the coarse concentration is high in summer and low in winter as expected from the increased summertime wind speed.

Figure 2, 3 and 4 presents the monthly average PM (chemically speciated) in coarse, accumulation and ultrafine mode respectively. In the coarse mode (Figure 2) metals and nitrate dominate and the overall emission levels are observed to be generally lower in winter. In the accumulation mode (figure 3) nitrate and OC dominates. The receptor sites have higher nitrate concentrations while the source sites (Downey and USC) have higher OC conc. High sulfate concentrations are observed at the receptor sites, especially during summer. In the ultrafine mode (figure 4), OC dominates. Increased wintertime OC concentrations at source sites are possibly due to condensable organics from vehicular emissions. Higher summertime OC at receptor sites is a result of secondary organic aerosol formation. Higher concentrations of EC at source sites is also observed suggesting primary emissions from diesel engines. Finally, overall sulfate concentration was observed to be low in ultrafine mode, but the concentration is higher in summer compared to winter due to its photochemical origin.

Figure 5 and 6 show the monthly average OC and EC distribution across the three different particle size modes. From figure 5, it can be seen that OC concentration is high in accumulation and ultrafine modes at source sites. At the receptor sites, higher summertime OC concentrations are observed for the ultrafine and accumulation modes, possibly due to increased photochemistry and advection. The monthly average EC distribution in the three modes (figure 6) reveals high EC at source sites resulting from diesel emissions. High concentration of EC in summer for ultrafine and accumulation at receptor site is also observed and can be explained by increased advection, which appears to overwhelm the extra dilution caused by the increased mixing height in the summer.

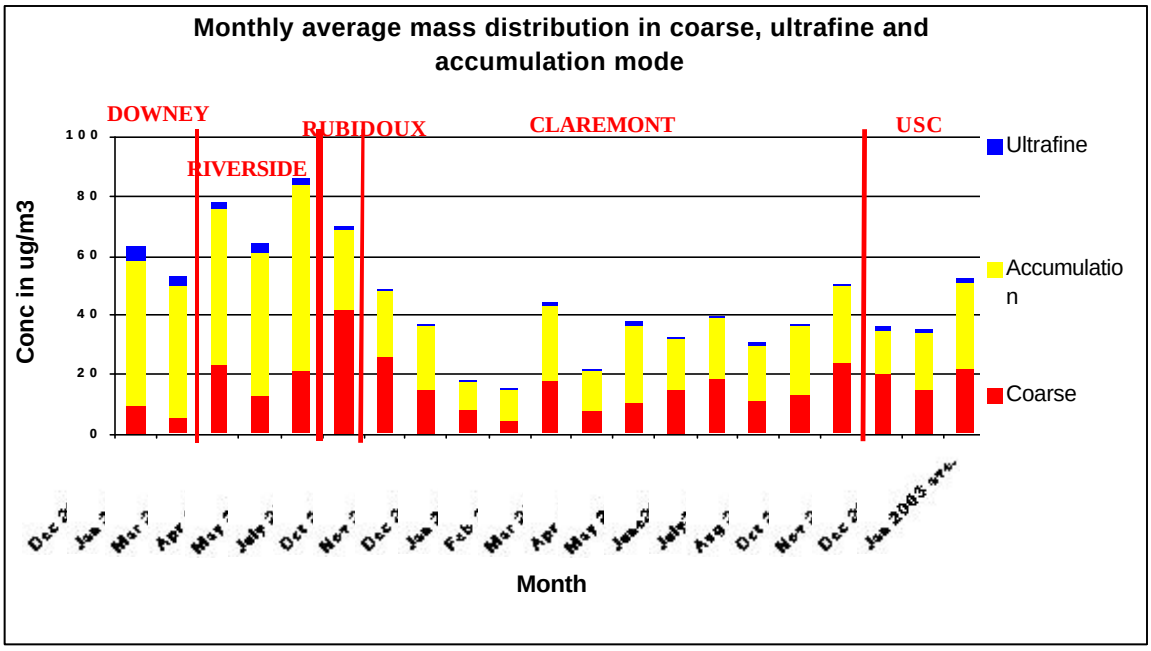

Figure1.

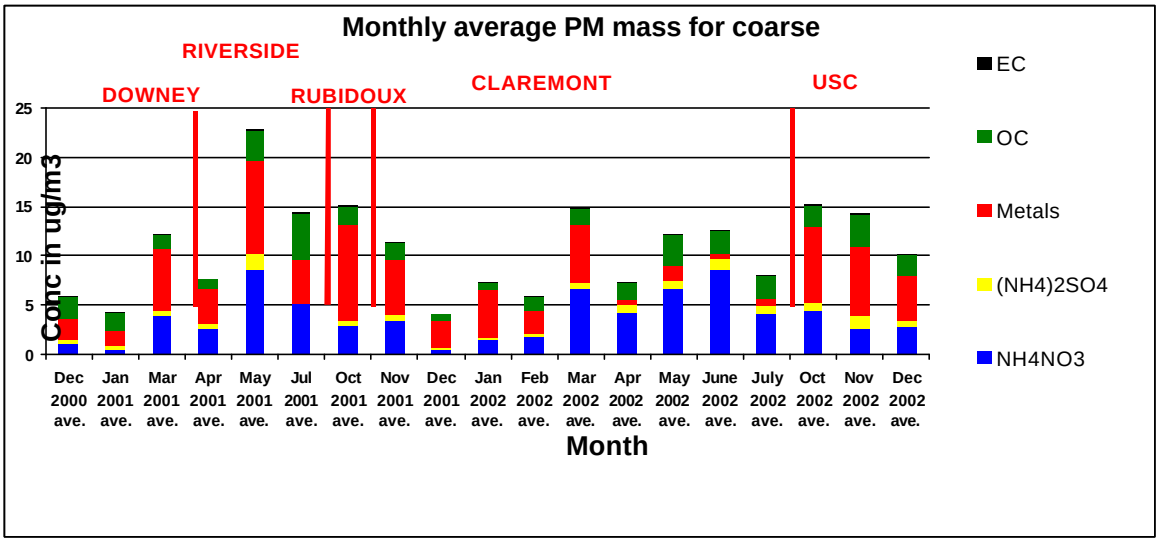

Figure 2.

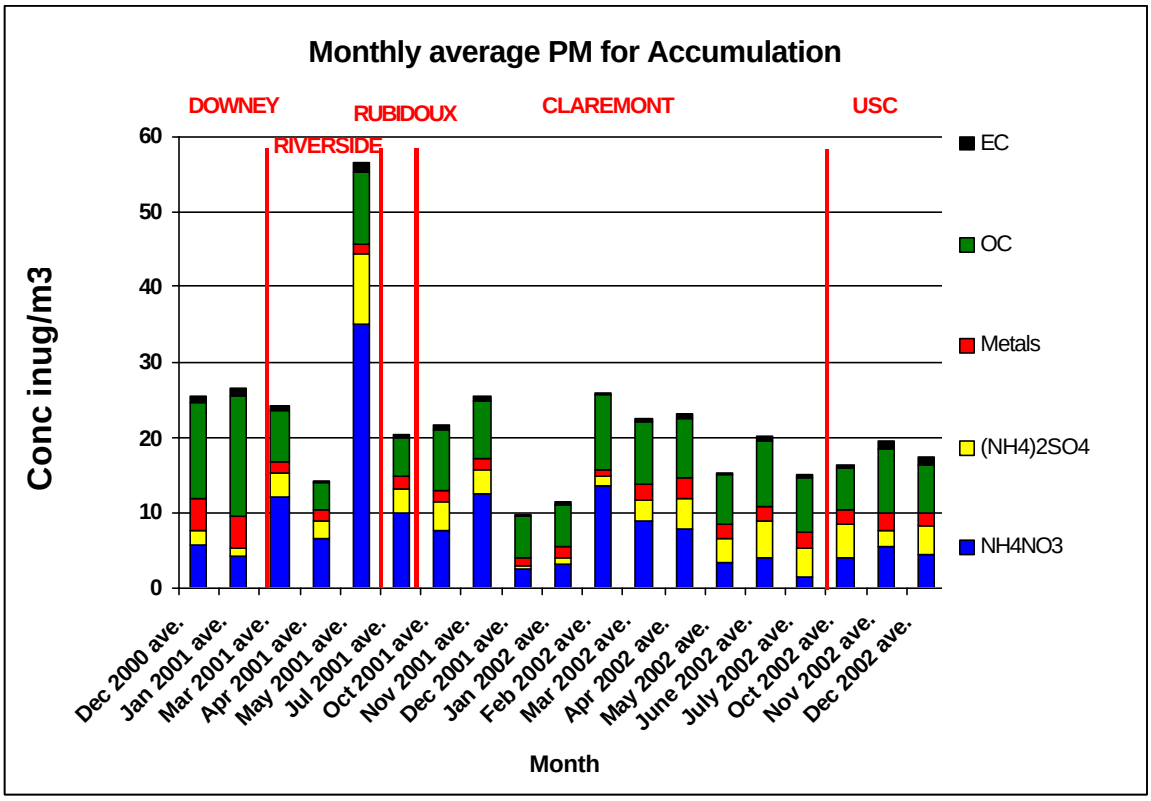

Figure 3

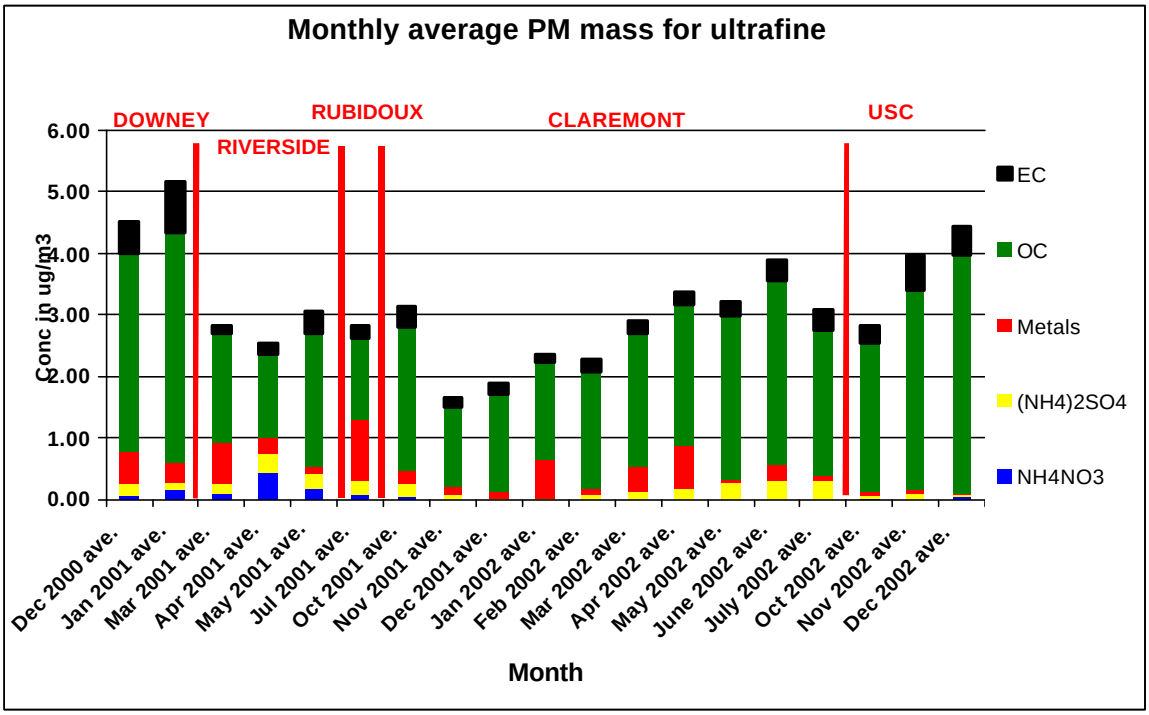

Figure 4

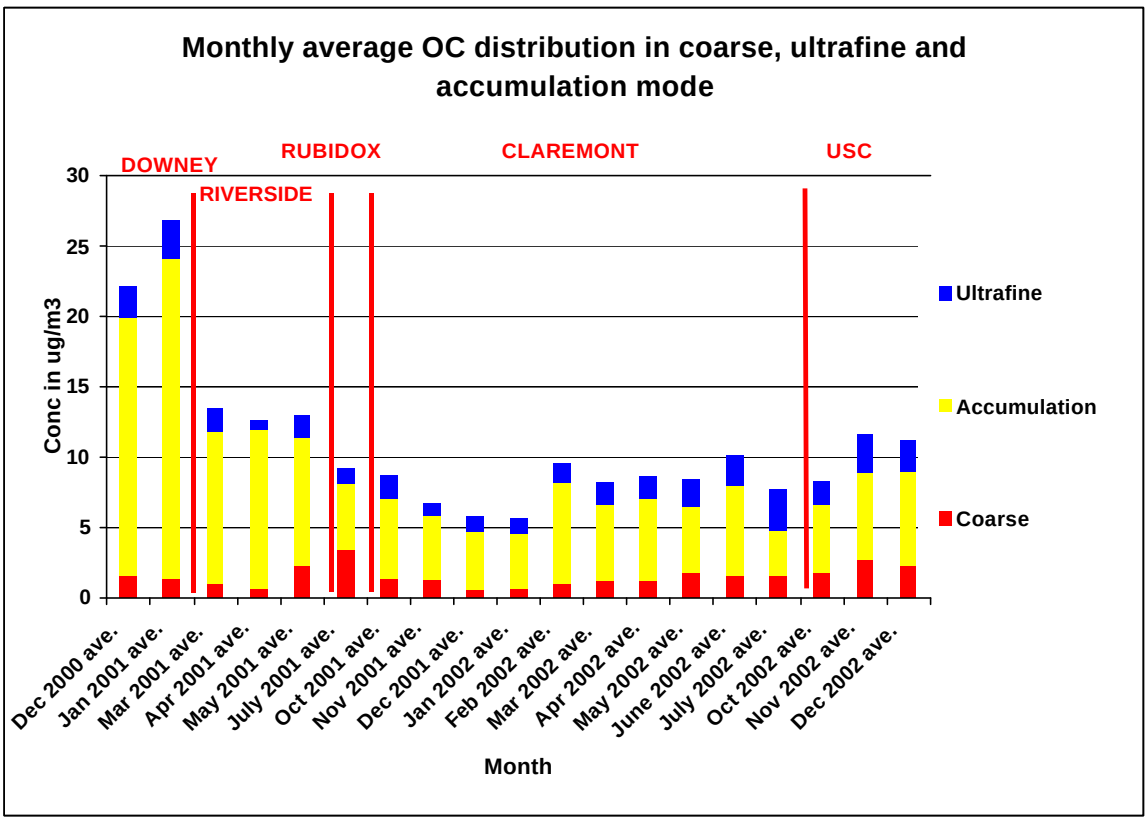

Figure 5

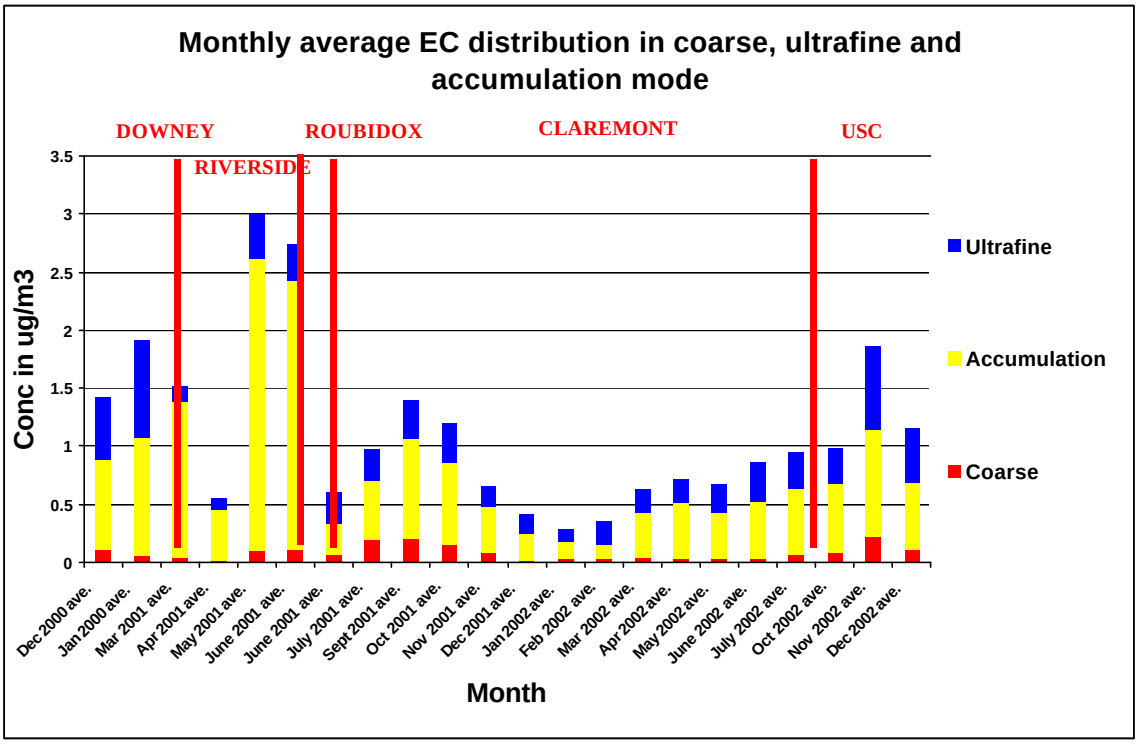
Monthly average EC distribution in coarse, ultrafine and accumulation mode
DOWNEY
ROUBIDOX
CLAREMONT
USC
RIVERSIDE
Conc in ug/m3
3.5
3
2.5
2
1.5
1
0.5
0
Ultrafine
Accumulation
Coarse
Dec 2000 ave.
Jan 2000 ave.
Mar 2001 ave.
Apr 2001 ave.
May 2001 ave.
June 2001 ave.
June 2001 ave.
July 2001 ave.
Sept 2001 ave.
Oct 2001 ave.
Nov 2001 ave.
Dec 2001 ave.
Jan 2002 ave.
Feb 2002 ave.
Mar 2002 ave.
Apr 2002 ave.
May 2002 ave.
June 2002 ave.
July 2002 ave.
Oct 2002 ave.
Nov 2002 ave.
Dec 2002 ave.
Month

Figure 6

6. Seasonal variation of the particle size distribution of polycyclic aromatic hydrocarbons and of major aerosol species in Claremont, California

This report summarizes the results and conclusions of a field study that has been written up and submitted for publication to ***Atmospheric Environment***, as part of the Supersite special issues.

Authors: Antonio H. Miguel*, Arantzazu Eiguren-Fernandez, Peter A. Jaques, John R. Froines, Bill L. Grant, Paul R. Mayo and Constantinos Sioutas

Summary

As part of the Southern California Particle Center and Supersite (SCPCS) activities, we measured, during all seasons, particle size distributions of twelve priority pollutant polycyclic aromatic hydrocarbons (PAHs), concurrently with elemental carbon (EC), organic carbon (OC), sulfate (SO_4^{-2}), and nitrate (NO_3^-) size distributions, from October 2001 to July 2002 in Claremont, CA, a receptor site located about 40 km downwind of central Los Angeles. Samples were collected approximately once every week, for 24-hr periods, from midnight to midnight. MOUDI impactors collected samples at 30 LPM which were composited for analysis into monthly periods in three aerodynamic diameter size intervals: 0-0.18 μm (ultrafine mode), 0.18-2.5 μm (accumulation mode), and 2.5-10 μm (coarse mode). For the monthly composites from October to February, the size distributions of the target PAHs are similar. However, from March to July, notable differences are observed: a significant fraction of the PAH mass is found in the coarse mode, as compared with the previous period. During the entire one-year period, the form and shape of the EC size distributions did not vary much and are distinguished by prominent mass in the ultrafine and accumulation size mode. For the individual modes of the major species, the highest Pearson correlation coefficients for the variation of temperature with species concentration were found in the ultrafine mode for both SO_4^2 (0.92) and EC (0.90), and in the coarse mode for both OC (0.85) and NO_3^- (0.54). High SO_4^{2-} correlations are consistent with increased gas-to-particle formation during the warmer months from SO_2 emissions in the Los Angeles seaport area and, similarly for EC, increased atmospheric transport to Claremont as the season progresses from winter to summer. While the correlations were all positive for the group of more volatile PAHs ($\log [p^oL] \geq -2.06$), although not statistically significant, they were all negative for the less volatile or particle-phase group ($\log [p^oL] \leq -3.22$), consistent with increased partitioning from the vapor-phase with decreasing temperature.

Conclusions

The effects of atmospheric transport on the size distribution of PAHs, EC, OC, SO_4^{-2}, and NO_3^- are reported, for the first time, during all seasons in a receptor site located about 40 km downwind of central Los Angeles. From October to February, the size distributions of PAHs are similar, but different from March to July, with increasing temperature and atmospheric transport. A significant fraction of the PAH and the NO_3^- mass moved towards the coarse mode, as compared with the previous period. The correlation of temperature with the concentration of all PAHs in the less volatile or particle-phase group (BAA-IND) was negative, consistent with increased partitioning from the vapor-phase with decreasing temperature. During all seasons, the form and shape of the

EC size distributions did not vary much and are distinguished by prominent mass in the ultrafine and accumulation modes. For the individual modes of the major species measured, the highest correlations were found in the ultrafine mode for SO_4^{2} (0.92) and EC (0.90). High positive correlation of sulfate with temperature in the ultrafine mode suggests increased gas-to-particle formation during the warmer months from SO_2 emissions in the Los Angeles harbor. High positive correlation of EC with temperature in the ultrafine mode suggests increased atmospheric transport of vehicular emissions from the urban downtown Los Angeles region.

7. Characterization of PAH and PAH-Derivatives

Introduction

The goal of our work is to characterize the polycyclic aromatic hydrocarbons (PAHs) and PAH-derivatives present at sites chosen to represent source sites or downwind receptor sites and to investigate the atmospheric chemistry occurring at these sites during different seasons. Of particular interest are nitro-PAHs and nitro-polycyclic aromatic compounds (nitro-PACs) since these compounds are potent mutagens and have been observed as products of gas-phase atmospheric reactions of PAHs. Since the last progress report, winter ambient sampling has been conducted in Los Angeles (at USC, January 13-17, 2003) and downwind at Riverside (agricultural operations site at UCR, January 27-31, 2003).

Status of Summer Samples. The filter samples from the summer field sampling have now been analyzed for nitro-PAHs and the data will be reported in the next progress report. This will complete analysis of the semi-volatile and non-volatile nitro-PAHs. Analysis of the volatile PAHs (Tenax samples) is complete, but analysis of the semi-volatile (collected on PUFs) and non-volatile (filter collected) PAHs remains to be done.

Status of Winter Samples. The Tenax samples for the volatile PAHs were analyzed as soon as possible after the actual sampling and, therefore, are completed. The filter samples from the winter field sampling are now being analyzed for nitro-PAHs. Remaining to be done: analysis of the semi-volatile nitro-PAHs and PAHs from the PUFs and analysis of the non-volatile PAHs from the filters.

Experimental section

Four time intervals per day were sampled during one week at Los Angeles (January 13-17, 2003) and Riverside (January 27-31, 2003). The daytime samples were 3.5 hours (morning 7 am-10:30 am, midday 11 am-2:30 pm and evening 3 pm-6:30 pm) and the nighttime sample was 11.5 hours (7 pm-6:30 pm).

The sampling sites were equipped with the following instrumentation: a Tenax solid adsorbent sampler, operating at 200 cm^3 min^{-1} for the daytime samples and at 100 cm^3 min^{-1} for the nighttime samples; two high-volume sampler with 2 polyurethane foam plugs (PUFs) located in series beneath a Teflon-impregnated glass fiber (TIGF) filter (20 cm $\times$ 25 cm) operated at ~0.6 m^3 min^{-1}. The analysis procedures were detailed in the September, 2002 quarterly report.

Each Tenax sample was spiked with deuterated internal standards and then thermally desorbed and analyzed individually by GC/MS. The values reported for the volatile PAHs for each time period are the average of the individual days.

Results

The maximum concentrations of the volatile PAHs in the winter samples were measured, (as in the summer samples) during the 0700-10:30 time intervals, but the winter concentrations were substantially higher than the summer values. For example, the naphthalene was 1583 ng/m^3 in the winter sample at USC compared with 391 ng/m^3 for the summer samples. In Riverside, the winter maximum was 536 ng/m^3, compared with a maximum of 300 ng/m^3 in the summer sample (see last progress report for tables of summer PAH values).

USC Average Ambient Concentrations of PAHs for January 13-17, 2003

	0700-1030 hr	1100-1430 hr	1500-1830 hr	1900-0630 hr
	ng/m^3	ng/m^3	ng/m^3	ng/m^3
Naphthalene	**1583**	**755**	**1202**	**1150**
2-MN	**728**	**310**	**581**	**642**
1-MN	**303**	**109**	**235**	**349**
Biphenyl	**22.5**	**14.7**	**14.1**	**21.0**
2-EN	**31.9**	**12.0**	**24.4**	**34.3**
1-EN	**4.5**	**2.1**	**3.4**	**4.9**
2,6/2,7-DMN	**41.2**	**14.0**	**34.0**	**56.4**
1,3/1,7-DMN	**41.7**	**13.3**	**33.5**	**60.1**
1,6-DMN	**19.5**	**6.9**	**15.9**	**29.1**
1,4-DMN	**3.4**	**1.6**	**2.7**	**5.2**
1,5/2,3-DMN	**10.0**	**3.8**	**8.9**	**15.4**
1,2-DMN	**7.2**	**2.8**	**6.2**	**10.2**

Key: MN = methylnaphthalene; EN = ethylnaphthalene; DMN = dimethylnaphthalene.

UCR Average Ambient Concentrations of PAHs for January 27-31, 2003

	0700-1030 hr	1100-1430 hr	1500-1830 hr	1900-0630 hr
	ng/m^3	ng/m^3	ng/m^3	ng/m^3
Naphthalene	**536**	**112**	**185**	**500**
2-MN	**285**	**48.6**	**78.8**	**237**
1-MN	**91.2**	**16.8**	**30.5**	**94.3**
Biphenyl	**10.5**	**5.4**	**5.5**	**11.0**
2-EN	**15.0**	**3.9**	**7.6**	**12.5**
1-EN	**2.4**	**1.5**	**1.2**	**1.7**
2,6/2,7-DMN	**18.2**	**4.4**	**7.7**	**17.8**
1,3/1,7-DMN	**16.8**	**3.9**	**6.7**	**16.9**
1,6-DMN	**9.2**	**2.3**	**4.0**	**9.4**
1,4-DMN	**2.3**	**0.8**	**1.3**	**2.0**
1,5/2,3-DMN	**5.0**	**1.4**	**2.6**	**5.2**
1,2-DMN	**3.5**	**1.1**	**1.8**	**3.1**

Key: MN = methylnaphthalene; EN = ethylnaphthalene; DMN = dimethylnaphthalene.

Manuscript Submission

A manuscript entitled "Methyl- and Dimethyl-/Ethyl- Nitronaphthalenes Measured in Ambient Air in Southern California" by Fabienne Reisen, Stephanie Wheeler and Janet Arey has been submitted for publication to ATMOSPHERIC ENVIRONMENT. Our ambient nitro-PAH data from the summer sampling at USC and UCR are described in this manuscript. The manuscript reports on environmental chamber reactions simulating ambient photo oxidation of volatilized diesel fuel PAHs and demonstrates for the first time that dimethylnitronaphthalenes (DMNNs) and/or ethylnitronaphthalenes (ENNs) identified as formed from the OH radical-initiated reactions of alkyl-PAHs present in diesel fuel are also present in ambient air samples collected in Southern California.

8. Coarse, Intermediate, and Fine PM Measurement

Introduction

During this quarter, data from a Continuous Coarse Monitor (CCM) was compared with a Scanning Mobility Particle Sizer-Aerodynamic Particle Sizer (SMPS-APS) tandem, an ESP differential Tapered Element Oscillating Microbalance (TEOM), and a PM2.5 Beta Attenuation Monitor (BAM). Both coarse and fine PM mass concentrations have been tracked each half hour. Data are downloaded about every two weeks from the CCM, SMPS-APS, and BAM. Rupprecht and Patashnick Co., Inc. download the ESP TEOM data periodically and share it with us, as it is available. Chemical and mass data from time-integrated samplers, including the MOUDI and Partisol, was analyzed and size modes were compared/contrasted. The intent of this work is to determine the relation between coarse PM (2.5-10 μm), intermediate mode PM (1.0-2.5 μm), and fine PM (0-2.5 μm).

Results

The intermediate PM mode mass concentrations were plotted against the coarse mode and PM_1 mass concentrations for Claremont, CA and USC. Figures 1-2 show the intermediate mode versus coarse and PM_1 modes, respectively, for Claremont. Figures 3-4 show the intermediate mode versus coarse and PM_1 modes, respectively, for USC. As evidenced by the figures, the intermediate mode correlates much better with PM_1 and not very well with coarse PM at both sites. An interesting observation is that the correlation between coarse and intermediate modes at Claremont jumps to 0.66 if the intermediate mode concentrations above 10 $\mu g/m^3$ are removed from the graph.

Figure 1. Intermediate Versus Coarse Mode PM in Claremont, CA

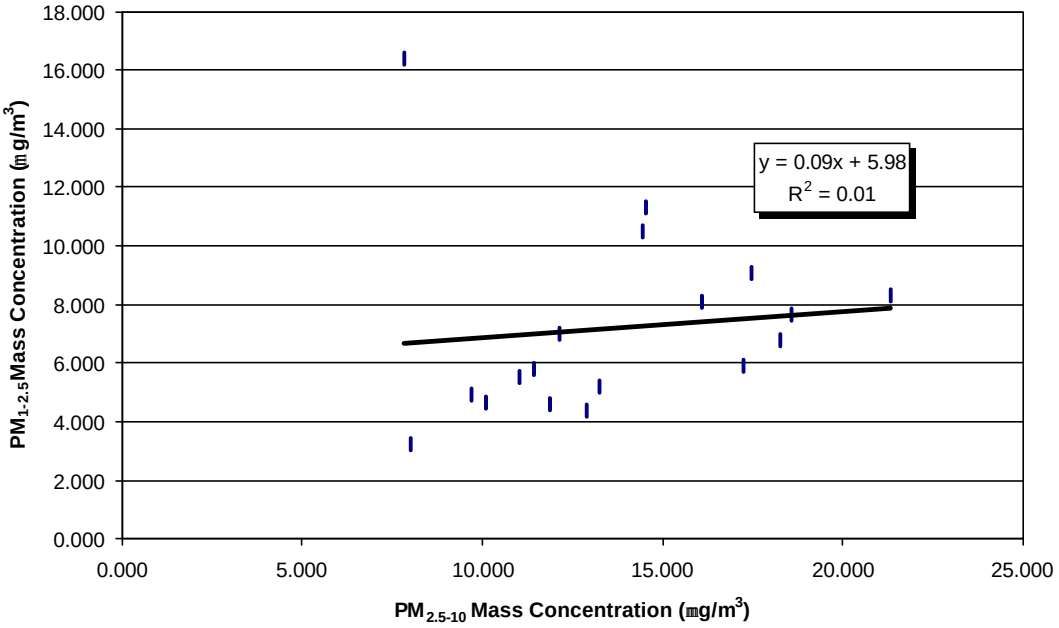

Figure 2. Intermediate Mode Versus PM_1 at Claremont, CA

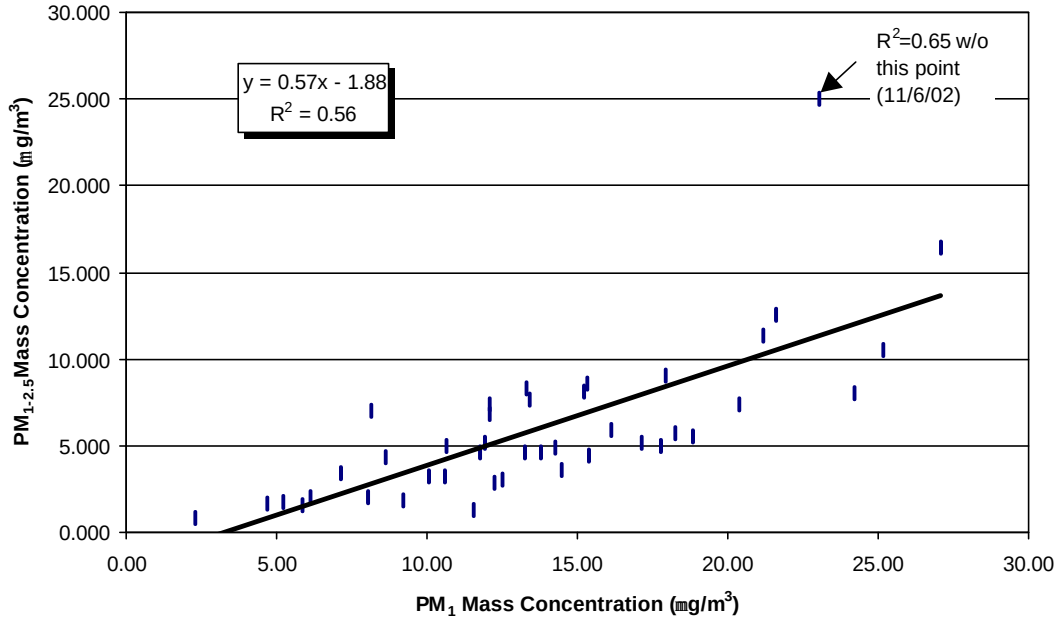

Figure 3. Intermediate Mode Versus Coarse Mode PM in Los Angeles, CA

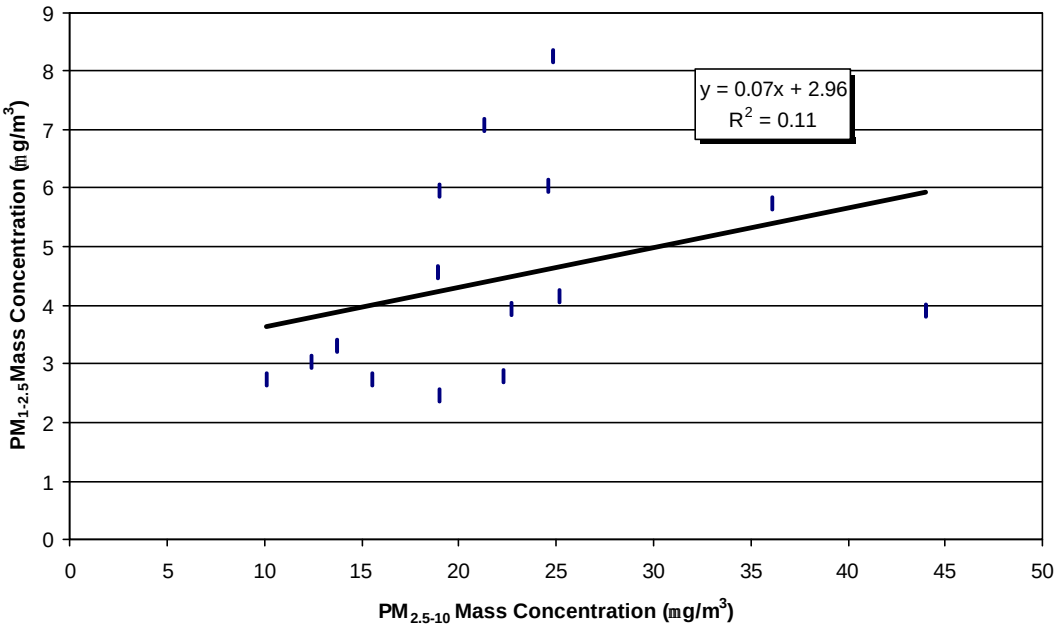

Figure 4. Intermediate Mode Versus PM_1 at Los Angeles, CA

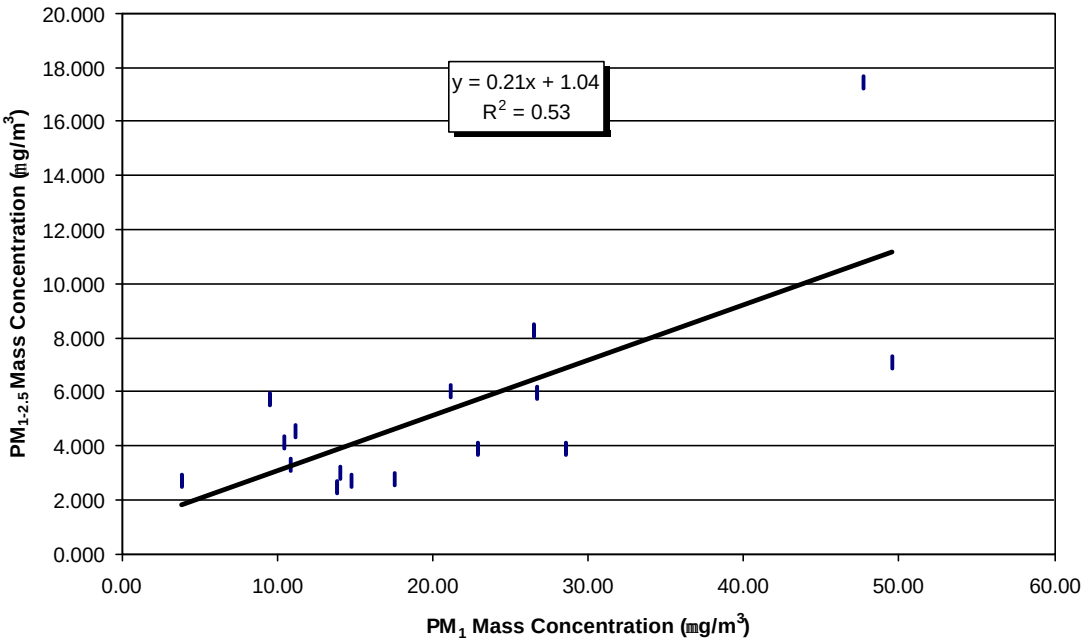

This is contrary to the belief that high coarse concentrations lead to high intermediate mode concentrations. If the tail of the coarse mode were affecting the intermediate mode, the higher mass concentrations of the intermediate mode would be expected to correlate with coarse mass concentrations for these events.

Problems

No large-scale problems were experienced during this quarter.

Next Quarter

Data has been collected from various instruments and sites. All data will be compiled and sorted in the next quarter with completion of this project occurring at the end of the next quarter. The focus of this study has shifted from continuous coarse and fine PM measurement to the comparisons between coarse PM, intermodal PM, and PM_1. The following data will be included in the final paper: chemical species data, continuous mass measurements, time-integrated mass measurements. Plots of mass concentrations versus time and versus other size mode mass concentrations will be presented in totality.

9. Predicting Ultrafine Particles near Major Freeways

Recent toxicology studies have demonstrated that atmospheric ultrafine particles are responsible for some of the adverse health effects. Motor vehicle emissions usually constitute the most significant source of ultrafine particles (diameter < 0.1 m) in an urban environment, yet, little is known about the concentration and size distribution of ultrafine particles in the vicinity of major highways.

The present research focuses on developing a model to determine ultrafine particle behavior after emissions, as they are transported away from the emission source --- a freeway. A major goal of this physical model is to characterize the atmospheric behavior of ultrafine particles by describing mathematically the spatial and temporal size distribution and relative concentration of ultrafine particles released from freeways into the atmosphere. Previously we observed rapid decrease in ultrafine particle number concentration and change in particle size distribution with increasing distance from freeways (Zhu et al. 2002a; Zhu et al. 2002b). Based on these experimental data, four sub-models, namely an atmospheric dispersion model, a coagulation model, a condensation-evaporation model and an adsorption model are being developed individually.

Atmospheric Dispersion

As a first step to modeling the concentration and size distribution of ultrafine particles in the vicinity of freeways, atmospheric dispersion model was developed based on Carbon Monoxide (CO) data that Zhu et al., (2002 a, b) reported. Since vehicular exhaust emission on the freeways is the major concern in the model, a line source emission model was adopted. Three models, the Gaussian Plume model, the Caline4 model and K-theory model were tested in this study. The K-theory with assumption that eddy diffusivity is a linear function of downwind distance turned out to the best and will be used to characterize the atmospheric dilution process near freeways.

Coagulation

Coagulation is one of the most important aerosol dynamic mechanisms in decreasing particle number concentrations and changing particle size distributions. The objective of the coagulation model is to simulate how ultrafine particle number concentration and size change as a function of distance from freeways. Vehicle emitted ultrafine particles often lie in the free-molecule regime and are in the form of fractal-like aggregates. Thus, fractal aggregates based coagulation kernels were used in this study.

Condensation and Evaporation

When a vapor condenses on a particle population or when material evaporates from the aerosol to the gas phase, the particle diameters change and the size distribution changes shape. For ultrafine particles near freeways, the condensation/evaporation species are most likely low-vapor-pressure Polycyclic Aromatic Hydrocarbons (PAHs) that were emitted from vehicles. Eiguren-Fernandez et al., (2003) reported gas- and particle-phase PAHs in six Southern California cities in different seasons (Eiguren-Fernandez et al. 2003). PAHs data from their study were used in the condensation/evaporation model.

Adsorption

Adsorption is a gas/particle partitioning process that changes particle size distribution. It differs from condensation in that adsorption leads to transfer of a fraction of the vapor to the aerosol phase, even if the gas phase is not yet saturated with the vapor (Seinfeld and Pandis 1998). Again, data from Eiguren-Fernandez et al., (2003) were used for the calculation in the adsorption model.

REFERENCES:

Eiguren-Fernandez, A., Miguel, A. H., Thurairatnam, S., Froines, J. R. and Avol, E. (2003). Spatial and Temporal Distribution of Vapor- and Particle-Phase Polycyclic Aromatic Hydrocarbons in Southern California Submitted to Environmental Science and Technology.

Seinfeld, J. H. and Pandis, S. N. (1998). Atmospheric Chemistry and Physics: from Air Pollution to Climate Change. Wiley, New York.

Zhu, Y., Hinds, W. C., Kim, S. and Sioutas, C. (2002a). Concentration and Size Distribution of Ultrafine Particles near a Major Highway. Journal of Air and Waste Management Assoc. 52:174-185.

Zhu, Y., Hinds, W. C., Kim, S., Shen, S. and Sioutas, C. (2002b). Study of Ultrafine Particles near a Major Highway with Heavy-duty Diesel Traffic. Atmospheric Environment. 36:4323-4335.

10. Chemical Characterization of Ultrafine Particles in the LA Basin

The plan for this study is to conduct bi-weekly MOUDI/Nano-MOUDI sampling in the following sites*:

Date	USC	Long Beach	Riverside	Upland
Fall	**Oct. 2-Oct. 16**	**Oct. 16-Oct. 30**	**Oct. 30-Nov.13**	**Nov. 13-Nov. 27**
Winter	**Feb. 27-Mar. 13**	**Mar. 13-Mar. 27**	**Jan. 27-Feb. 13**	**Feb. 13-Feb. 27**
Spring	**Apr.1-Apr.14**	**Apr.15-Apr.28**	**Apr. 29-May 12**	**May 13-May 26**
Summer	**July 15-July 28**	**July 29-Aug.11**	**Aug.12-Aug.25**	**Aug.26-Sept.8**

***Shaded dates indicate completed and/or in progress.**

Introduction

Aluminum substrates were pre-baked and sealed prior to January 27, 2003. Six substrates per two-week period were used. The MOUDI/Nano-MOUDI combination was employed at each site listed above from January 27, 2003 to March 27, 2003. The winter sampling will conclude after the submission of this report. Sampling was non-stop for the listed periods with no change of substrates except between sites. The only exception to this was a two-hour period at USC when sampling was shut down due to work on the roof in close proximity to the MOUDI's. Upon completion of each site's sampling, the substrates were split into two pieces. Three-fourths were sent to Tony Miguel (UCLA) for organics analyses, and one-fourth was sent to Rancho Los Amigos for ion chromatography. The chemical analyses for the fall sampling period have been completed with results shown below.

Results

The following figures show the elemental carbon (EC) and organic carbon (OC) concentrations as a function of particle size collected. Figures 1-4 represent data obtained from USC, Long Beach, Riverside, and Upland, respectively. USC displays the highest ultrafine PM carbon concentrations. Riverside has the second highest levels of carbon in the larger ultrafine size ranges (56-180) while Upland is second to USC in the 0-56 nm ultrafine carbon concentrations. For the most part these results are expected because USC is a source site while Riverside and Upland are receptor sites. During this time of this particular year, photochemistry contributed very little to ultrafine particle production because of abnormally cool and cloudy weather. Also, rain and wind events were present during this sampling period. Thus, receptor sites had very low ultrafine particle concentrations. The mass concentration size distributions for the winter period have not been presented herein because they are similar to those of the previous report. Also not presented are the ion chemical date (sulfate, nitrate) because no observable levels of these compounds were detected in the 0-56 nm size range.

Problems

Some of the measurable masses on the aluminum substrates in the 10-32 nm range are at or close to the detection limits. The MOUDI and NanoMOUDI impaction plates are becoming clogged, resulting in increased pressure drop and decreased flow rates. They will be cleaned thoroughly before the next phase of sampling begins.

Next Quarter

The next phase of sampling will occur in what is the spring season in the LA basin. The same four sites will be visited from April to June. EC/OC and ion chemical data will be available for the winter season.

Figure 1. USC EC/OC Fall 2002

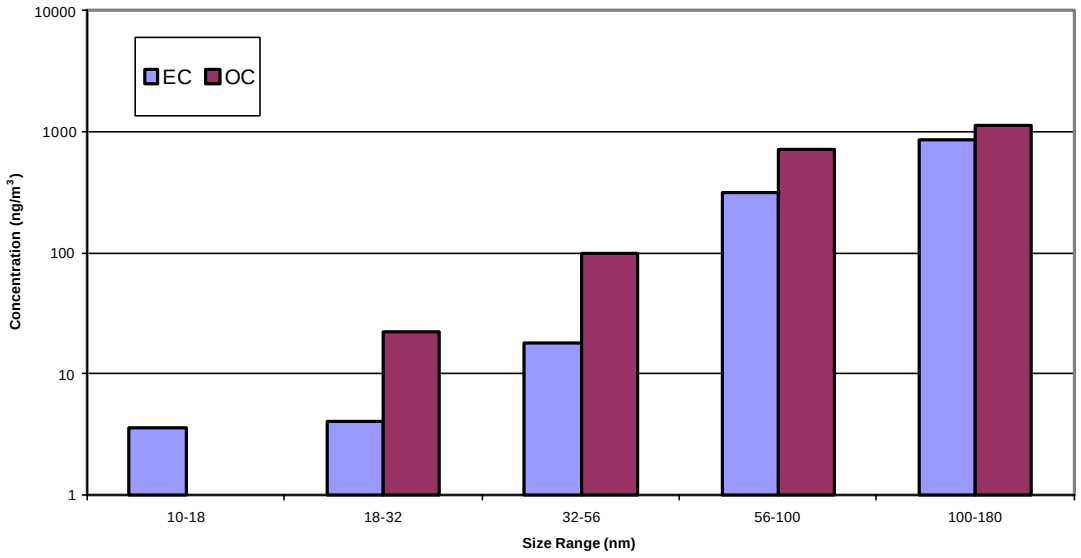

Figure 2. Long Beach EC/OC Fall 2002

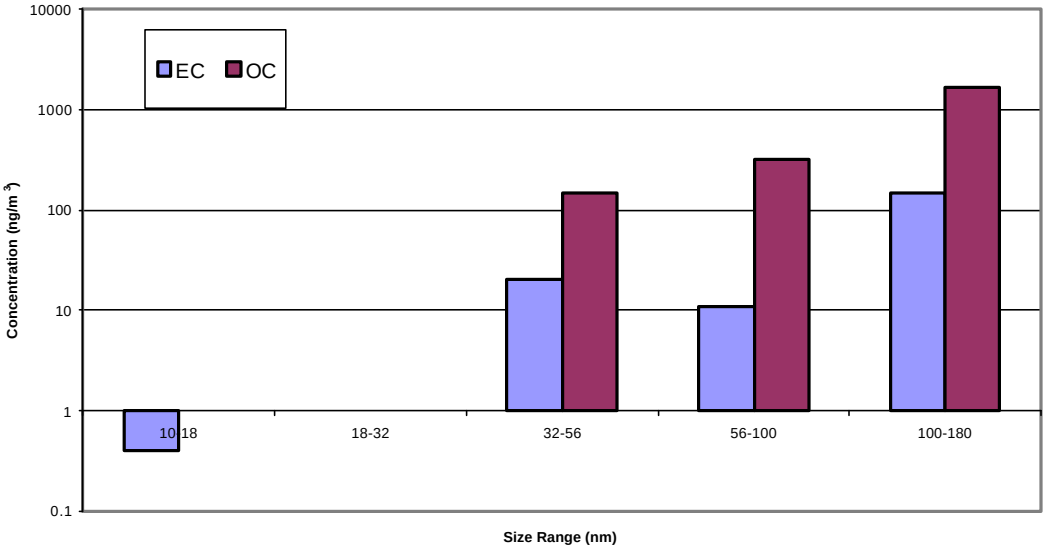

Figure 3. Riverside EC/OC Fall 2002

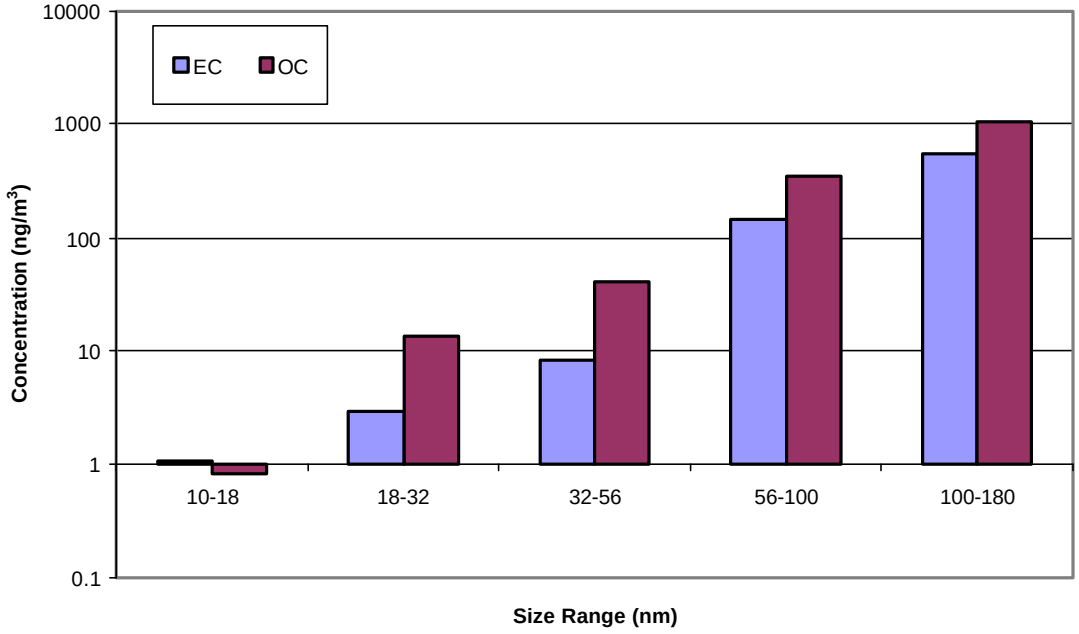

Figure 4. Upland EC/OC Fall 2002

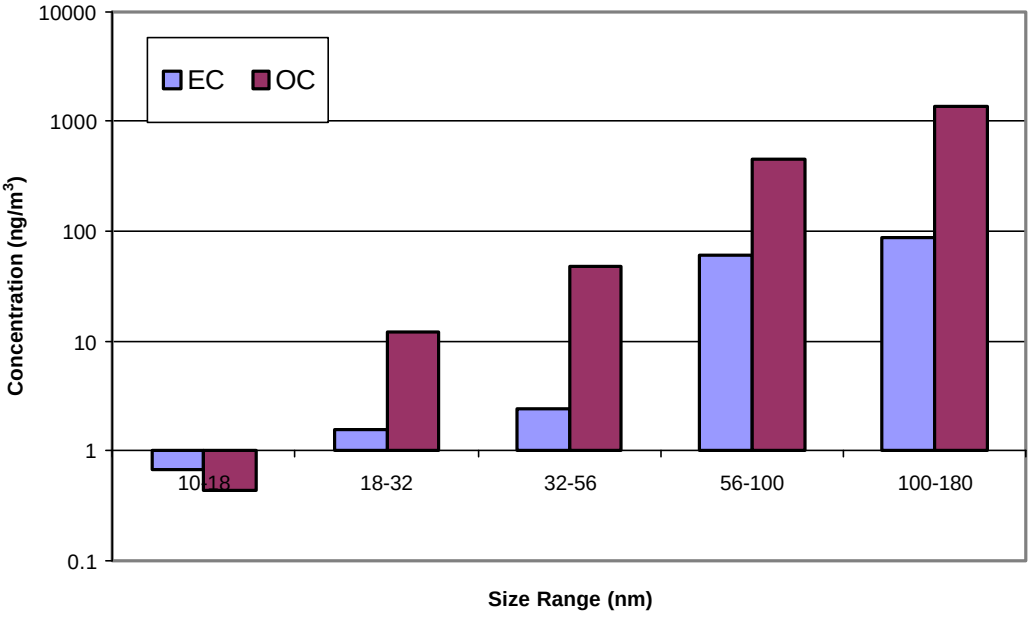

11. Ultrafine Organic Speciation Study

Several studies have measured individual organic compounds in atmospheric particle samples by GC/MS or other analytical methods. Usually, only between 10 and 20% of the total organic compound mass (measured by thermal desorption methods) can be quantified as individual organic species. Some of these compounds can be used to trace primary particle emissions and be used in source apportionment studies. One of the major hurdles in the sampling of particles for organic speciation is collecting enough mass for the analysis. For this reason, sampling periods are very long (from 12 hours to several days) and they do not provide size-fractionated information on the organic particle concentrations. The one study that measured size-fractionated speciated organics only looked at PAH and oxy-PAH and sampled over 5 - 24 hour periods (J. Allen et al., 1996,1997, 1998).

A new particle slit impactor developed by Dr. Sioutas and his group (Misra et al., 2002) through funding by the Southern California Supersite enables the separation of particles with a cut point of 0.18 m and a very high flow rate of ~500 lpm. Using a 2.5 m inlet, particles with diameters between 0.18 m and 2.5 m (fine) can be collected by impaction on this new impactor, and particles with diameters less than 0.18 m (ultrafine) can be collected on a high-volume filter downstream. The two size fractions roughly correspond to the accumulation mode and ultrafine modes of the urban aerosol size distribution. The high flow rate of the system allows for shorter collection periods, and thus diurnal (3 ½- hour samples) and size-segregated sampling for organic speciation is now possible.

The sampling plan outlined below has recently been completed. Briefly, two sampling sites were selected: a typical urban site (USC); and a downwind receptor site (Riverside). For one week at each site (Mon. – Fri.), four time intervals per day were sampled (morning, midday, evening, and possibly overnight). The daytime samples last 3 1/2 hours per day for each diurnal interval for five days. Nighttime sampling lasts for 11 1/2 hours per night for four nights. Filters and substrates are replaced in the sampler such that one set of accumulation mode quartz-fiber substrates and one ultrafine mode high-volume Teflon-coated glass fiber filter represent a weekly average for each diurnal interval. Parallel to the high volume sampler was a MOUDI run at 30 lpm to collect particles on Teflon substrates for mass and ion chromatography. The stages in the MOUDI will be chosen to correspond to the same cut-points as the high volume sampler. A second MOUDI with the same flow rates and size cuts collected aluminum foil substrates and a quartz fiber after filter for EC/OC analysis by the thermal desorption/optical transmission method used regularly by the Supersite. In addition, a 47mm filter train will consist of a PM2.5 cyclone inlet, a Teflon filter and a back-up quartz fiber filter. The flow rate will be chosen to create a face velocity on the quartz back-up filter equal to the face velocity on the MOUDI quartz after filter. This filter-based sampling helps to assess the degree of organic vapor adsorption onto the MOUDI quartz after filter.

An additional high volume sampling system, operated by Janet Arey's UCR group, consisted of a filter followed by a PUF and will be used for analysis of both semi-volatile and particle-phase PAH, oxy-PAH and nitro-PAH.

The purpose of this project is several-fold. First, with the exception of the one study on PAH and oxy-PAH, the speciated organic composition of ultrafine particles has not been investigated. Several other classes of compounds, including alkanes, substituted phenols, alkenes, alkanoic acids and diacids, aromatic carboxylic acids, resin acids, sugars and furans have been found in atmospheric particles but their distribution among size fractions is unknown. Ultrafine particles consist of fresh particles emitted directly from sources, freshly condensed material on these primary particles, and freshly nucleated particles resulting from atmospheric reactions. It has also been shown that ultrafine particles consist of up to 80% - 90% organic carbon. Source profiles for many of the organic compounds of interest have been previously determined for the most important particle sources in Los Angeles (Schauer Thesis, 1998). Furthermore, smog chamber studies have identified many particle phase organic atmospheric reaction products that should also be found in the atmosphere.

By comparing individual ultrafine organic species to known organic source profiles and expected atmospheric reaction products, the sources and formation mechanisms of these ultrafine particles can be determined. Recent data suggesting that ultrafine particles may be more toxicologically potent than larger particles provide even more motivation for this study. Identifying the origin, the geographical distribution, and the diurnal and seasonal variations of these particles will help to model personal exposure and to formulate any future pollution control efforts. By also looking at the organics on the accumulation-mode filter sample, the contributions of primary particle sources and secondary organic aerosol to the two particle size fractions can be resolved over the course of the day, as air parcels move across the LA basin, and as atmospheric conditions change with season.

Finally, the warm weather and large number of pollution sources in the LA basin create ideal conditions for secondary organic aerosol (SOA) formation. A goal of this study is to identify individual components of SOA in order to provide a chemical signature that can estimate the degree of SOA contribution to ambient particle mass concentrations. The temporal and spatial aspects of this study will shed additional light on SOA formation mechanisms.

Experimental Matrix

- Two sites: Urban (USC), and Receptor (UC Riverside)
- One week (five days) at each sampling site for each season
- Four time intervals each day: 7AM - 10:30AM, 11:00AM – 2:30PM, 3PM –6:30PM, and 7:00PM – 6:30AM
- Weather conditions and traffic patterns should remain constant throughout each week, and preferably, throughout the entire study.
- When: August, to maximize effect of photochemistry; and January, a low photochemical and cold weather sample

Progress

The sampling phase of this study has been completed. From August 12 to August 16, 2002, sampling was conducted on the rooftop of a 3-story building at the University of Southern California campus (urban site). From August 26 to August 30, 2002, sampling took place at the

University of California, Riverside Citrus Research Center and Agricultural Experiment Station (CRC-AES) adjacent to an existing SCAQMD air sampling facility (receptor site). Sampling at the same two locations was repeated to obtain wintertime samples. Winter USC sampling occurred from January 13-17, 2003 and Winter Riverside sampling took place from January 27-31, 2003.

Analysis for particle mass based on the MOUDI Teflon substrates are shown in the following figures. In the summer, PM2.5 mass peaked midday at USC and in the morning at Riverside. The winter samples showed the highest PM2.5 and ultrafine concentrations at USC in the morning, which may be due to the wintertime inversion level that increases in altitude over the course of the day. Winter in Riverside was characterized by high PM2.5 levels overnight. At both sites during the summer, ultrafine PM mass was higher in the midday and evening than the morning or overnight. This pattern was repeated in Riverside during the winter, however, USC in winter showed the highest ultrafine levels in the morning. Also note that ultrafine levels at USC were generally higher in the winter than in the summer. In both seasons, ultrafine mass concentrations were higher in Riverside than at USC, suggesting a photochemical origin above primary contributions from vehicular emissions.

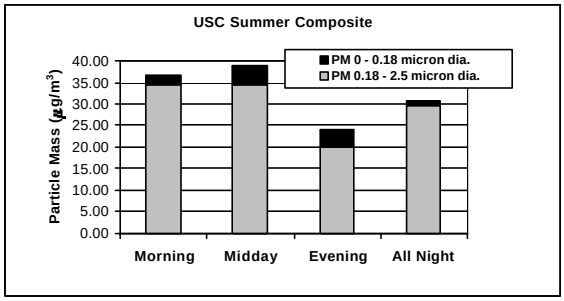

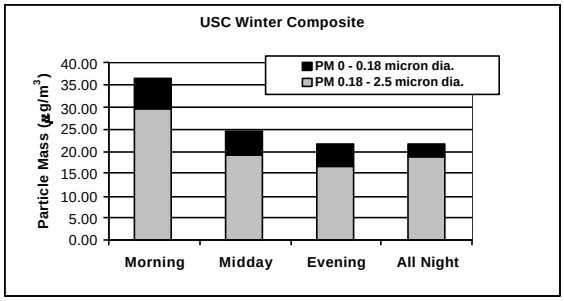

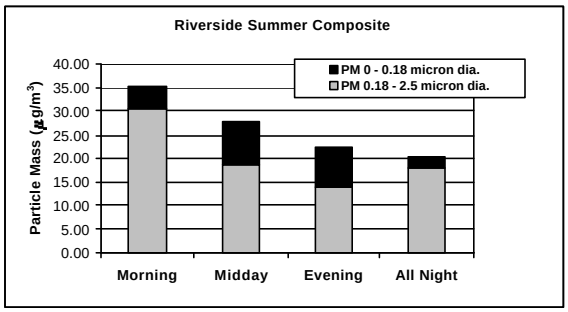

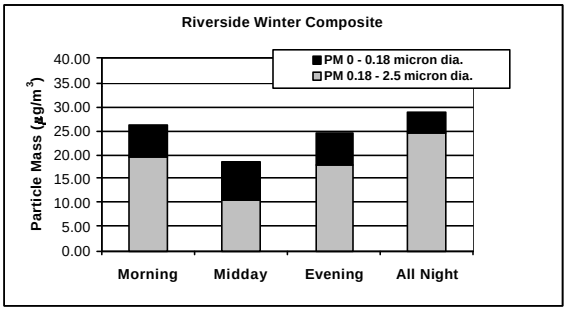

Organic carbon and elemental carbon analysis have been completed for the summer and winter samples and are currently being evaluated. Organic speciation by GC/MS and inorganic analysis by ion chromatography are underway and nearing completion.

12. Continuous PM 2.5 Mass by the Differential TEOM® MONITOR and a Continuous Size Segregated Nitrate Monitor in Claremont California: Evaluation of the Dynamics of Nitrate Volatilization

As part of the Los Angeles based U.S. EPA sponsored Southern California Particle Center and Supersite (SCPCS), semi-continuous (10-minute) particulate matter less than 2.5 micrometers (PM2.5), and semi-continuous (10-minute) size segregated particulate nitrate (2.5-1.0 μm, 1.0-0.5 μm, & 0.5~0.1 μm) were measured using the Differential TEOM® monitor (Patashnick, et al., 2000; Jaques, et al., 2002; October 2002 Los Angeles Supersite quarterly report), and a cascaded Integrated Collection and Vaporization Cells (ICVC) (Stolzenburg, et al., 2002; Fine, et al., 2002), respectively. The Differential TEOM monitor employs an electrostatic precipitator to resolve artifactual changes in filter mass change related to semi-volatile PM. The electrostatic precipitator (ESP) is activated in alternating 5-min periods to remove particles from the sample air stream. The mass change of the filter with the ESP activated is subtracted from the mass change during the normal collection (with the ESP off) to provide an artifact-corrected mass. The results presented are part of a poster that is to be presented at the Particulate Matter: Atmospheric Sciences, Exposure and the Fourth Colloquium on PM and Human Health in Pittsburgh (March 31-April 4, 2003), and submitted to the meeting's special issue proceedings in May 2003. The full data to be presented will be from the SCPCS Claremont site.

The primary hypothesis that we are testing is that the rate of ammonium nitric acid and ammonia gas volatilization from particle-bound ammonium nitrate that is loaded on the TEOM's fiber filter varies as temperature increases, and as relative humidity, PM-mass, particle-nitrate mass, aerosol size, and pre-existing filter loading decreases. Routine PIU metrics available are 10-minute ICVC nitrate, 5 minute Differential TEOM mass, including 10-minute ESP on and off data, SMPS-APS 15-minute, and MOUDI 24-hr size fractionated mass that corresponds to the ICVC sizes. The model, below will be used to test that the predicted rate of volatilization follows the net mass measured by the Differential TEOM's "ESP on" cycle, which represents the period where particles are not sampled, and thus, includes mass lost or gained by either, or both, volatilization and adsorption, respectively. The semi-continuous "ESP on" data will be compared to the predicted volatilized nitrate for two primary sets of conditions: 1) episodes of high nitrate, where nitrate dominates the PM-associated mass; and 2) low PM events where nitrate tends to predominate. These ambient events measured at the Claremont site will be compared to that of theory (e.g., Zhang and McMurry; 1987, 1991, and 1992; and Cheng et al., 1997), and to lab measurements (e.g., Furuuchi et al., 2001, and Schwab et al., 2003) – all which primarily consider the evaporation of pure ammonium nitrate from fibrous filters. Furuuchi, measured the evaporation of lab generated PM-nitrates from a non-Differential TEOM after flushing the filter with particle free air.

The following equation may be used to estimate the loss of evaporated HNO3 + NH3, which will be compared to the total evaporated mass from the differential TEOM (i.e., the ESP-$_{on}$ phase);

$$M_e = 2M_d - \left[\left(\frac{\Delta P}{P_\circ - \Delta P}\right)(2.583)\left(\sqrt{K}\right)\right] \qquad \text{(Eq 1)}$$

M_e represents the estimated evaporated HNO3 + NH3, and M_d represents the total mass delivered to sampler substrate [i.e., in the case of pure NH4NO3, either (ESP-$_{on}$ – ESP-$_{off}$), or ICVC NO3]. DP = Pressure drop through the sampler, which is determined from empirical measurements made by the Differential TEOM, and P_0 is atmospheric pressure.

The above model is derived from that of Zhang and McMurry (1987, 1991, and 1992), which assumes saturated conditions above and below the filter, and is derived from the efficiency of the filter to maintain an equilibrium between particle mass and the vapors associated with specific PM, as follows:

Filter efficiency can be described as a function of the pressure drop, and gas to particle concentrations, as

$$\eta_e = \frac{1}{\left[1+\chi_f \frac{r_s}{C_m}\right]}$$

where η_e = sampling collection efficiency of volatile particles for filters, or as a function of the relationship of the total delivered mass M_d to total evaporated mass M_e, as

$$\eta_e = 1-\frac{M_e}{M_d}$$

$\frac{r_s}{C_m}$ = ratio of equilibrium gas-phase concentration, at saturation conditions, averaged over the sampling period to the measured aerosol mass concentration.

For time-integrated periods,

$\overline{r_s} = \int_0^t r_s(t)dt/t$, in µg/M^3

$= \sqrt{K}\left(MW_{HNO_3}\right)(B)$, where

$\left(MW_{HNO_3}\right)$ = Molecular Weight of HNO_3
= 63

B = Conversion factor
= 0.041

K = Dissociation Constant for $NH_4NO_3 \Leftrightarrow NH_3 + HNO_3$, Mozurkewich (1993)

Note: see Cass et al., 1983; and, Stelson and Seinfeld; Atmos Env, 1982, to determine NH4NO3 deliquescence curve for different temperatures.

For RH Below the deliquescence point,
Ln(K) = 118.87 – 24084/T – 6.025ln(T), (Mozurkewich; Atmos Env, 1993)

For RH above the deliquescence point,
$K^* = [P_1 - P_2(1-a_w) + P_3(1-a_w)^2](1-a_w)^{1.75}K$, where

a_w = RH

P_1, P_2, and P_3 are defined in the citation.

$$x_f = \frac{\Delta P}{h(P_0 - \Delta P)}$$

x_f = dimensionless pressure drop for TEOM filter

h = sampling efficiency for non volatile particles = 1

P_0 = Sampler upstream pressure (ambient)

= 1 Atmosphere

ΔP = Pressure drop through sampler

So as to estimate the volatilized HNO3 and NH3, we can set the filter efficiency terms to be equivalent, as

$$h_e = \frac{1}{\left[1 + x_f \frac{r_s}{C_m}\right]} = 1 - \frac{M_e}{M_d}$$

Solving for M_e gives

$$\frac{M_e}{M_d} = 1 - \frac{1}{\left[1 + \chi_f \frac{r_s}{C_m}\right]}$$

$$M_e = M_d \left\{1 - \frac{1}{\left[1 + \chi_f \frac{r_s}{C_m}\right]}\right\}$$

Substituting for χ_f,

$$M_e = M_d \left\{1 - \frac{1}{\left[1 + \left(\frac{\Delta P}{(1-\Delta P)}\right)\frac{r_s}{C_m}\right]}\right\}$$

Substituting for $\overline{r_s}$

$$M_e = M_d \left\{1 - \frac{1}{\left[1 + \left(\frac{\Delta P}{(1-\Delta P)}\right)\frac{\left(\sqrt{K}\left(MW_{HNO_3}\right)(B)\right)}{C_m}\right]}\right\}$$

substituting values

$$M_e = M_d \left\{1 - \frac{1}{\left[1 + \left(\frac{\Delta P}{(1-\Delta P)}\right)\frac{2.583\sqrt{K}}{C_m}\right]}\right\} \qquad \text{(Eq. 2)}$$

at RH < deliquescence point

C_m = measured Nitrate aerosol mass concentration by the ICVC system
M_e = total evaporated mass (ESP_{on}); and

M_d = total Nitrate mass (i.e., ambient) delivered to sampler substrate
ΔP = Pressure drop through sampler, and
Ln(K) = 118.87 – 24084/T – 6.025ln(T)

M_e is now computed in terms of the empirical outcomes measured at the PIU

$$\eta_e = 1 - \frac{M_e}{M_d} = \frac{C_m}{C_{mo}}, \text{ (Zhang \& McMurry; 1991; Env Sci Tech)} \qquad \text{(Eq 3)}$$

where C_m and C_{mo} = measured and true atmospheric PM, respectively

Assuming that $M_d = C_{mo}$ (i.e., that the mass ambient mass is all delivered to the filter),
And substituting M_d for C_{mo}, gives:

$$C_m = M_d - M_e \qquad \text{(Eq 4)}$$

Substituting into Eq 2, gives:

$$M_e = M_d \left\{ 1 - \frac{1}{\left[1 + \left(\frac{\Delta P}{(1 - \Delta P)} \right) \frac{2.583\sqrt{K}}{M_d - M_e} \right]} \right\}$$

Solving for M_e, gives:

$$M_e = 2M_d - \left[\left(\frac{\Delta P}{P_\circ - \Delta P} \right) (2.583) \left(\sqrt{K} \right) \right] \qquad \text{(Eq 1)}$$

where units for K is ppb^2, and for P is inches-H_20; P_0 = 1 atmosphere (ambient)

Variables from the PIU that are needed to compute M_e:

1) M_d = Ambient NO3 by ADI measurements;
2) Sampling T and RH conditions – T is 30 Deg-C, then this is a constant for K; if for both the lab and field experiments, we need to know whether RH is below the deliquescence point to determine which formula for K we use.
3) ΔP, which is derived from the TEOM's frequency data.

Results and Discussion

Herein, we compare the mass lost during the "ESP-on" cycle to ambient particulate nitrate concentrations measured by the ICVC. For measurements at Claremont, episodes of PM2.5 are often highly associated with ammonium nitrate, and they generally correspond with high daytime temperatures, peaking during mid-afternoons. Figure 1 presents continuous ambient Differential TEOM and NH4NO3 data for a 3-day period in February at Claremont. The peak PM2.5 mass and NH4NO3 coincides with daytime high temperatures.

Figure 2 presents lab results using the Differential TEOM to measure polydisperse NH4NO3 onto a new filter (Schwab et al., 2003). Aerosol was sampled for about 8 hours, followed by filtered air. The hourly average PM2.5 mass data is the difference between the ESP off and on cycles. The off cycle represents activity without PM collection, when the kinetics of volatilization can be observed. Once filter loading develops, during the first couple hours, volatilization can be seen by observing the ESP-on trend increase in negative mass, and then once the PM filter mass has stabilized, the negative ESP-on mass becomes lower. Once aerosol free air is sampled, the ESP-on mass asymptotes to zero over a 9 hour period. Table 1 defines the time periods for the changes in mass concentrations (net ESP, and ESP on/off) – for the purpose of evaluating saturated and non-saturated dependent volatilization phenomenon. "Equation 1" will be used to evaluate the saturated conditions present during these measurements, and a similar algorithm, derived from the experiments of Furuuchi (2001) to predict the NO3 lost during the particle free period of this experiment.

The dynamic processes of adsorption and volatilization vary with numerous conditions (e.g., meteorology, and sources). Thus, it is best to evaluate the process of Nitrate loss from the Differential TOEM filter under ideal conditions that don't exist in the complex mixture of PM that prevails in the Los Angeles basin. Conveniently, during several occasions, Nitrate events dominate PM episodes, and these are best to evaluate NO3 loss from its filter, with minimum artifact confounders. Figure 3 presents two PM episodes (a and b) that are high in particulate matter as measured by the Differential TEOM, and high in PM2.5 NO3, as measured by the ICVC system. The cumulative ICVC NO3 mass, and sampling condition of the Differential TEOM will be compared to the measured "ESP-on" (i.e., mass-lost) results by using "Equation 1", assuming saturated conditions (Zhang and McMurry, 1987, 1991, & 1992). For non-saturated conditions (see Figure 3d, where PM is moderate, but predominantly NO3), the same parameters will be applied to a similar algorithm based on that by Furuuchi (2001). Most of the high PM dominated by NO3 occurred in the winter time at Claremont, while during the warmer months, much of the PM during episodes was high in non-nitrate pm, that often was adsorbing in nature (e.g., see Figure 3c).

Since the volatilization of NO3 can be reflected by the ESP on measurements, especially during a PM episode high in NO3, we are evaluating the relationship of ICVC NO3 to the ESP on cycle. We plan to test our hypothesis that the volatilization rate is dependant on NO3 and mass particle size. Figures 4 presents a set of scatter plots of the 10-minute ESP-on mass versus the NH4NO3 for PM2.5 and the 3 size fractions of the ICVC system. For PM2.5, the negative slope of -0.46 and high correlation of 0.75, clearly show that desorption occurs from the filter with ambient NH4NO3

collection. If should be noted, though, that the 5-minute ESP-on and –off cycling protocol subtracts out these artifact effects (Jaques, et al., 2002). Time delayed TEOM data (maximized at 40 minutes) vs real time NH4NO3 also suggests delayed volatilization effects. The best association is for PM2.5, and less so, although highly correlated, for the separate size fractions. Additional size fractionated analysis will be conducted for non-saturated conditions. Also, size fractionated Differential TEOM PM2.5 ESP-on and net mass data will be estimated, based on co-located measurement by the SMPS-APS and MOUDI, to do size fractionated correlations of the Differential TEOM with NO3 by the ICVC system.

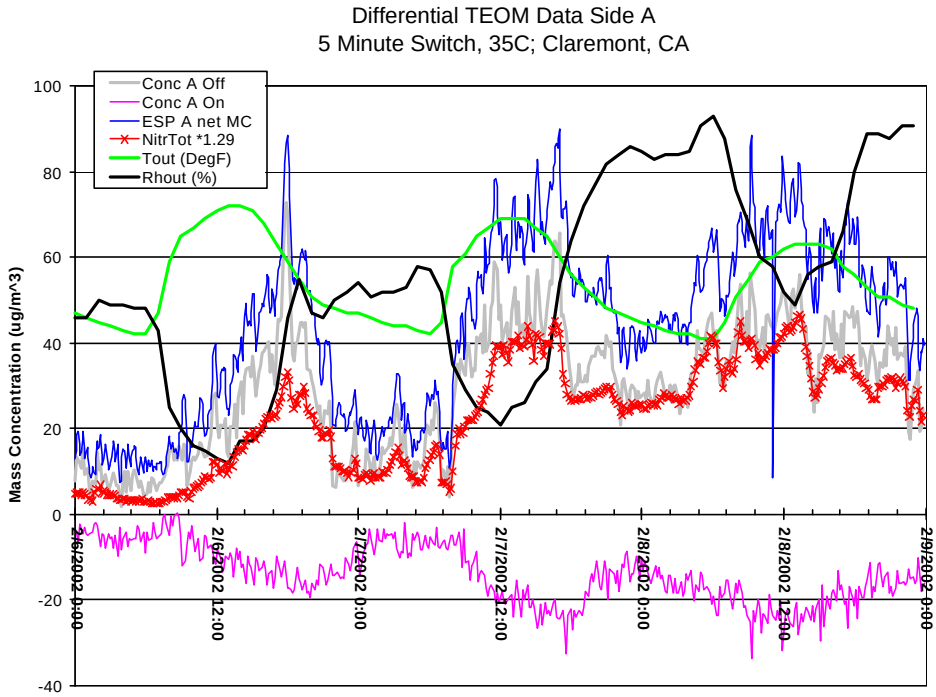

Figure 1. selected 5 minute Differential TEOM mass data with the ESP on and off, compared with 10 minute PM2.5 Ammonium Nitrate measured by the ADI system for a 3-day period during February 2002 – with Temp and RH data.

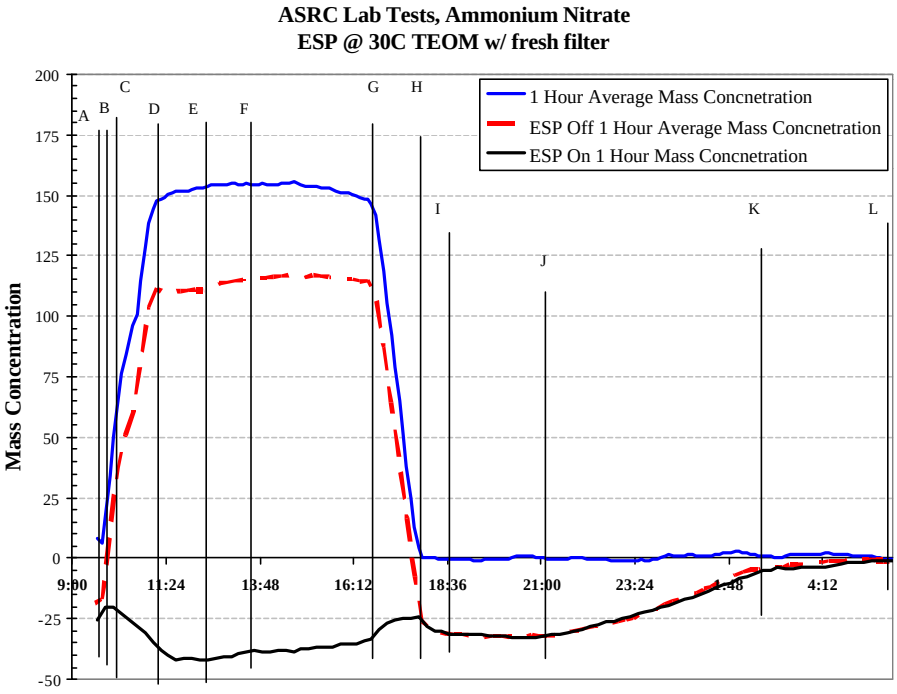

Figure 2. Laboratory tests of Differential TEOM, evaluating the kinetics of Ammonium Nitrate volatilized from the filter.

Table 1. Concentration changes for TEOM mass parameters by time period.

Period	Time	Net Mass Conc.		ESP off		ESP on	Comments
A-B							
	9:45-	from: +6.447 to	9:45-	from -17.04 to			
B-D	11:09	+147.87	11:09	+111.42			
					9:51-	from: -19.89 to -	
B-C					10:03	20.53	
					10:03-	from: -20.53 to -	
C-D					11:15	38.04	
	11:09-	from: +147.87 to	11:09-	from: +111.42 to	11:15-	from: -38:04 to -	
D-E	12:21	+152.87	12:21	+110.48	12:27	42.27	ESP-on Non-linear
	12:21-	from: +152.87 to	12:21-	from: +110.48 to	12:27-	from: -42.27 to -	
E-F	13:33	+154.62	13:33	+116.35	13:39	38.11	
	13:33-	from: +154.62 to	13:33-	from: +116.351 to	13:39-	from: -38.11 to -	
F-G	16:33	+148.30	16:33	+114.73	16:39	33.46	
	16:33-	from +148.30 to	16:33-	from: +114.73 to -	16:38-	from: -33.46 to -	
G-H	17:57	+0.270	17:57	26.02	17:51	24.35	ESP-on Non-linear
	17:57-	from: +0.270 to -	17:57-	from: -26.02 to -	17:51-	from: -24.35 to -	
H-I	18:33	0.451	18:33	31.11	18:39	31.25	ESP-on Non-linear
	18:33-		18:33-	from: -31.11 to -	18:39-	from: -31.25 to -	
I-J	21:09	from: -0.451 to -0.079	21:09	32.05	21:15	31.74	
	21:09-		21:09-		21:15-	from: -31.74 to -	
J-K	2:33	from: -0.079 to +1.00	2:33	from: -32.05 to -4.8	2:39	5.9	
	2:33-		2:33-		2:39-	from: -5.9 to -	All values at about zero
K-L	5:33	from: +1.00 to +0.54	5:33	from: -4.8 to -1.86	5:39	0.910	ug/m3

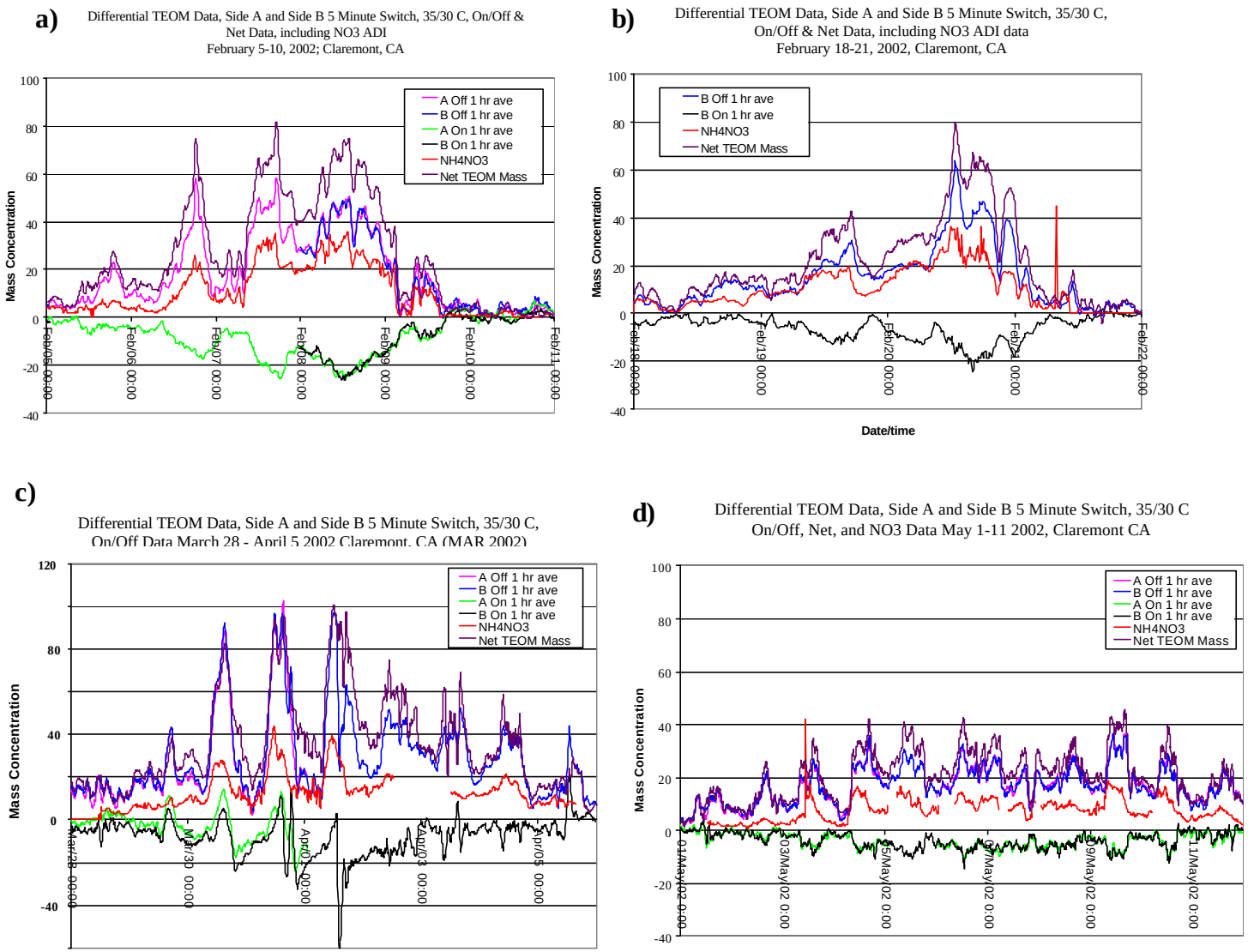

Figure 3. a) and b) PM episodes consisting mostly of nitrate; c) PM episode with nitrate, but higher in adsorbing material; and d) summer period with moderate, but consistent PM, that is mostly nitrate.

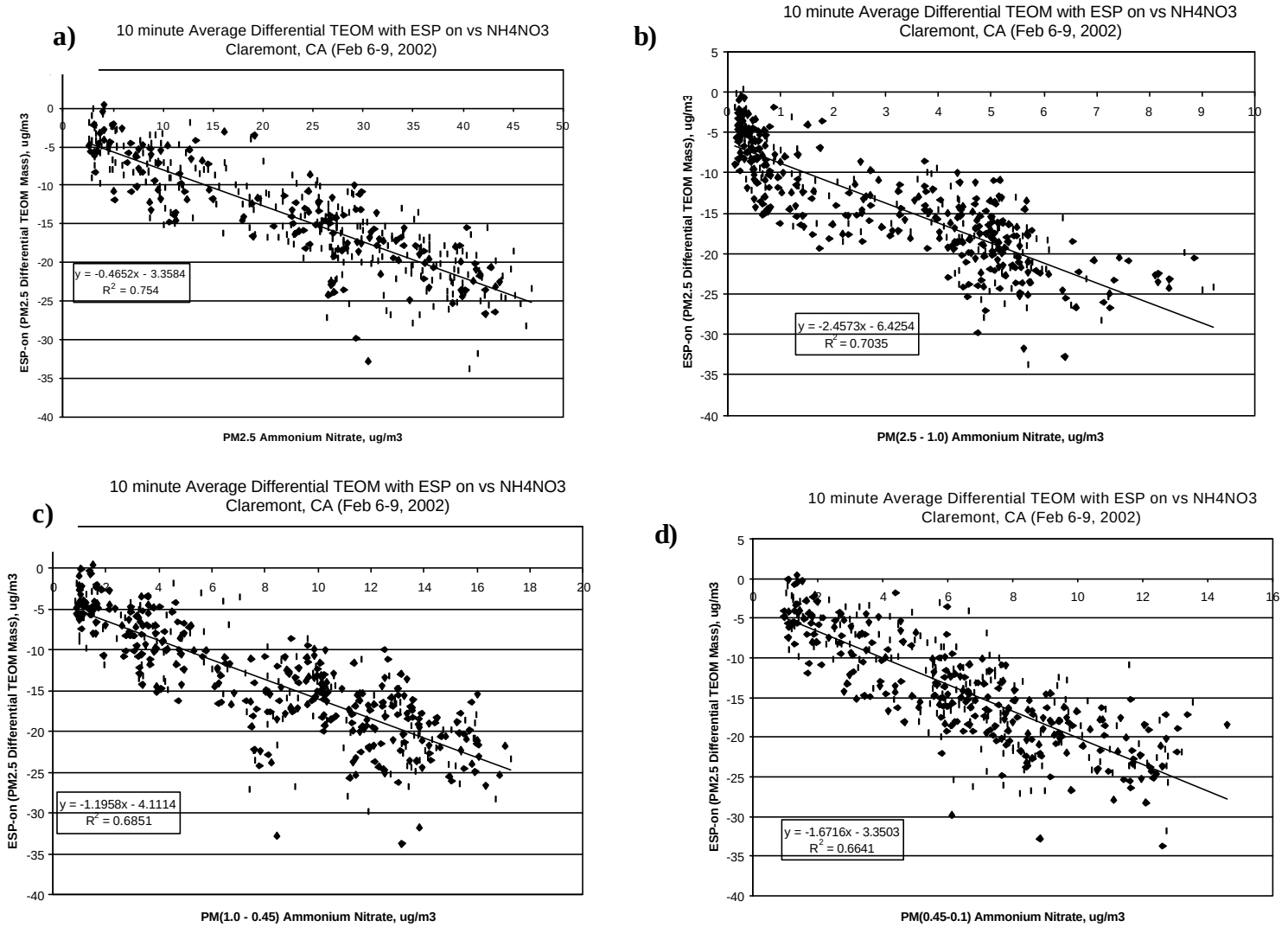

Figure 4.. Scatter plots of 10-minute averaged Differential TEOM data with the ESP on versus size fractionated NH4NO3 data for February 6-9, 2002 at Claremont, CA

13. Performance Evaluation of an active personal DataRAM $PM_{2.5}$ mass monitor (Thermo Anderson pDR-1200) designed for continuous personal exposure measurements

INTRODUCTION

Exposure to ambient particulate matter (PM) has recently received considerable attention as the result of epidemiological findings showing associations between ambient particulate concentrations and mortality (Ozkaynak and Thurston, 1987; Schwartz and Dockery, 1992; Dockery et al., 1993; Pope et al., 1991 ; Katsouyanni et al. 1995; Pope et al., 1995). Several studies have indicated that outdoor and even indoor concentrations may be poor estimators of personal exposures to PM_{10} or $PM_{2.5}$ and its components.
The objective of the study presented in this paper was to evaluate the usefulness of an active flow, personal DataRAM (pDR, Model 1200; MIE Inc., Bedford, MA) for providing real-time mass concentration measurements and to assess the effect of particle size and humidity on the relationship between the response of the pDR and the actual aerosol mass concentration. The active pDR, like previous DataRAM models, is an integrated nephelometer that measures continuously the amount of light (with wavelength, l, equal to 880 nm) scattered by particles drawn though a sensing zone at a flow rate of 4 lpm. The amount of light scattered is converted to particle concentration readings using well-established light scattering theory (Kerker, 1969) and factory calibrations. In this paper, we present results from a field evaluation of this instrument conducted in Southern California from December 6, 2002 to February, 19, 2003. The performance of the active pDR was compared to other collocated continuous and time-integrated PM2.5 samplers.

METHODS

The active pDR (shown schematically in Figure 1) is an integrating nephelometer (scattering coefficient range = 1.5 x 10-6 to 0.6 m-1 at wavelength 880nm). It has maximum external dimensions of 153 mm (6.0 in) H x 92 mm (3.6 in) W x 63 mm (2.5 in) D, weighs 0.5 kg and operates in a temperature range of -20° to 70° C and relative humidity range from 10 to 95%. It records in units of mg/m3, as calibrated by the manufacturer using a fine ISO test dust (specific gravity, 2.5, d_p50 = 2-3 µm). For this study, the pDRs were programmed to record 15 min averages. The pDR is preceded by a metal cyclone (BGI model GK 2.05) with a cut point of 2.5 µm at 4 lpm, designed specifically for $PM_{2.5}$ monitoring. An advantage of using the pDR is active mode is the ability to easily attach a filter holder for 37 mm filters directly downstream of the photometric sensing chamber. The filter can then be analyzed for mass or chemical composition much like the time-integrated personal monitors mentioned in the previous section. In the current experiment, Teflon membrane filters (PTFE, 2 µm pore, Gelman Science, An Arbor, MI) were deployed for concurrent gravimetric measurements of the aerosol mass concentration for comparison to the continuous electronic measurements provided by the instrument. Air samples were drawn through each pDR by means of a lightweight, personal pump (BGI 400S Personal Sampling Pump, Waltham, MA).

Three identical active pDR units with corresponding personal pumps were placed inside an instrumentation trailer located near the University of Southern California in downtown Los Angeles as part of the activities of the Southern California Particle Center and Supersite. In this current setup, outdoor air is first pumped through a Model TE-6001 Inlet (SSI) (Tisch Environmental Inc, Cleveland, OH), similar to those used in high-volume air samplers for routine

monitoring. The ambient aerosol then is drawn through the roof of the trailer via a stainless-steel tube which then branches into three sampling lines, each leading to one of three pDR units for simultaneous outdoor air sampling. Each of the three pDRs operates at a flow of 4 lpm and is preceded by a $PM_{2.5}$ cyclone described above. Before each experiment, the DataRAM was calibrated following standard calibration procedures recommended by the manufacturer. These include zeroing of the instrument (i.e., testing with particle-free air provided by a filter supplied by the manufacturer) and span checking (i.e., a secondary calibration which is performed using a built-in optical scattering/diffusing element). This internal calibration ensures that before each test started, the calibration factor was reset to the manufacturers laboratory calibration. This factor can be adjusted by the user to account for differences between the calibration dust used by the manufacturer and ambient aerosol.
Time-integrated $PM_{2.5}$ sampling was conducted in simultaneous 24-hour runs using a Partisol sampler (Model 2025 Sequential Air Sampler, Rupprecht and Patashnick Co. Inc., Albany, NY; Patashnick et al., 2001) and the pDR back-up filter to determine total $PM_{2.5}$ mass on 24-hour basis. Teflon filters for both the Partisol sampler and the back-up pDR filter holders were pre- and post-weighed using an MT5 Microbalance (Mettler Toledo Inc, Highstown, NJ). Relative humidity was measured every 15 minutes by a thermo hygrometer, HI-9161F (Hanna Instruments, Italy).

The pDR continuous $PM_{2.5}$ concentrations are compared with those measured by a collocated Beta Attenuation Monitor (BAM, Model 1020, Met One instruments, Inc., OR), preceded by a size selective inlet of $PM_{2.5}$.

RESULTS AND DISCUSSION

Precision of the Active pDR monitors

The precision of the collocated pDR monitors for measurement of the ambient $PM_{2.5}$ mass concentration was found to be very high. Figures 1a and b illustrate the degree of correlation found among the three collocated pDRs. The three pDR readings were highly correlated with r^2 greater than 0.99 and slopes within ± 10% of unity in all cases. In our collocated precision tests, the pDRs were not necessarily zeroed regularly in order to simulate actual field operations and to account for bias due to potential operation error with respect to zeroing. Thus, these results may more accurately represent actual field operation of the monitors. The results shown in Table 1 also confirm the excellent agreement among the three pDR.
Figure 2 displays a one-week time series of the collocated pDR data, averaged every two hours to correspond to the BAM measurements also shown in the figure. Again, excellent agreement among the three pDR monitors is observed, indicating very high precision. The BAM measurements track the pDR readings over the first two days, but then deviate significantly until the last day of the week when good agreement is observed again. Note than even when the absolute concentrations differ, the trends of the pDRs are matched to some degree by the BAM. The four days when the two types of instruments do not agree were characterized by high relative humidities (exceeding 80%). Due to the excellent degree of precision among the pDR monitors, the average of the three pDR readings is used for all subsequent comparisons to other particle measurements.

Table 1. Summary Statistics of the Comparisons Between the 2-hr and 24-hr $PM_{2.5}$ Concentrations Obtained by pDR, BAM and Partisol

Instruments Compared	N	Geometric Mean of Ratios	Mean Relative Difference	p-Value
Continuous Comparison				
PDR1 vs. pDR2	**573**	**1.029**	**0.133**	**0.299**
PDR1 vs. pDR3	**559**	**1.023**	**0.135**	**0.163**
PDR2 vs pDR3	**564**	**1.015**	**0.089**	**0.323**
Average pDR vs BAM (All RH)	**206**	**1.33**	**0.165**	**< 0.001**
Average RH-Corrected pDR vs BAM (RH > 60%)	**111**	**0.97**	**0.189**	**0.31**
Average pDR vs BAM (RH < 60%)	**95**	**0.98**	**0.161**	**0.11**
Gravimetric Comparison				
PDR1 vs. pDR2	**20**	**1.027**	**0.071**	**0.367**
PDR1 vs. pDR3	**20**	**1.004**	**0.080**	**0.387**
PDR2 vs pDR3	**20**	**1.032**	**0.105**	**0.485**
Average pDR vs Partisol	**20**	**1.027**	**0.117**	**0.391**
Average Gravimetric pDR vs 24-Hour BAM	**20**	**1.112**	**0.170**	**0.089**
Average 24-Hour Electronic pDR vs Average Gravimetric pDR	**20**	**1.528**	**0.79**	**0.001**
Corrected Average RH-Corrected 24-Hour pDR vs. Average Gravimetric pDR	**18**	**1.058**	**0.325**	**0.129**
Average BAM vs. Partisol	**20**	**0.92**	**0.13**	**0.11**

pDR/BAM inter-comparison and humidity effects

Table 1 also presents results of the inter-comparison between the average of the three pDR readings (averaged over two-hour time periods) and the two-hour BAM monitor output, which we use as a reference for $PM_{2.5}$ concentrations. With a geometric mean pDR to BAM ratio of 1.33 (± 0.56), the pDR reads significantly ($p<0.001$) higher particle levels than the BAM. For data corresponding to ambient relative humidities exceeding 60%, the pDR to BAM concentration ratio increases to 1.71 (± 0.68). Previous studies have shown that light scattering particle measurement devices are subject to error at high relative humidities (Sioutas et al, 2000; Day et al., 2000). A previous evaluation of a stationary DataRAM (also manufactured by Mie, Inc.)

showed that the DataRAM technology over estimates particle concentrations at relative humidities (RH) over about 60% (Sioutas et al, 2000). Figure 3 plots the pDR/BAM ratio as a function of two-hour average relative humidity. The results are very similar to the previously reported stationary DataRAM performance (Sioutas et al, 2000) with the ratio increasing almost exponentially above an RH of 60%. The model fit included on Figure 3 is based on an empirical correction factor (CF) described by the Laulainen (1993):

$$CF=1+0.25RH^2/(1-RH) \quad (1)$$

where RH is the relative humidity. This model was also shown to fit more recent data presented by Day et al. (2003) quite well. As Figure 3 indicates, the modeled particle growth predicted by that equation fits the actual field data well with a correlation coefficient of 0.88.

Figure 4 graphically displays the relationship between the average pDR and BAM $PM_{2.5}$ concentrations at times when the RH was less than 60%. Very high correlation between the measurements is observed ($r^2 = 0.87$). The two hour averaged $PM_{2.5}$ concentrations determined by pDR and BAM are also in excellent agreement with each other, with the pDR-to-BAM ratio being 0.98 (± 0.16), as indicated in Table 1. As already demonstrated in Figure 3, agreement between pDR and BAM measurements is not expected for RH above 60%. However, by correcting the pDR readings when the RH was greater than 60% with the empirical relationship described in equation (1), the two measurements can be brought into reasonable agreement. Table 1 also demonstrates the effectiveness of this correction, with an uncorrected pDR to BAM ratio of 1.71 (± 0.68), compared to a corrected concentration ratio 0.97 (± 0.19). Further analysis showed that the RH-adjusted pDR and BAM concentrations are not statistically different ($p = 0.31$).

Particle Size Effects

The effect of the particle size on the pDR response was investigated by calculating the mass median diameter (MMD) as determined by concurrent measurements of size distributions using a tandem SMPS and APS system. The variation of the pDR/BAM ratio as a function of MMD is shown in Figure 5. By only considering time periods when the RH was less than 60%, the confounding effects of RH described above are eliminated. Certain data points are also excluded when the SMPS/APS system appeared to be malfunctioning (during the period between January 2 to 5, 2003). The experimental data follow the classic trend predicted by the Mie scattering theory (Kerker, 1969), with an overestimation of particle mass between about 0.7 and 1.2 mm MMD. The observed pattern, as well as the best fit third order polynomial curve shown in Figure 5, agree remarkably well with previously reported results of a stationary DataRAM by Sioutas et al (2000). It is known that variations in particle size introduce considerable errors in predicting the response of a nephelometer (Sioutas et al, 2000, Thomas and Gebhart, 1994). The intensity of scattered light from an individual particle increases from about 0 (for very small, ultrafine particles) to a maximum value at a particle size that corresponds to approximately 1.25 times the wavelength of the incident light. The pDR uses a light source with wavelength of 0.88 mm, hence maximum scattering should be observed at about 1.1 mm particles. Note that, as shown in Figure 5, this is the approximate MMD value where the pDR over estimates the BAM measurements to the greatest degree. For refractive indices in the range of 1.4-1.6 (i.e., those of the most common $PM_{2.5}$ components), light scattering will decrease quite sharply at either larger or smaller particle sizes.

Since the pDRs were calibrated using ISO fine test dust (MMD 2-3 μm, sg =2.5, as aerosolized) the instrument response to a finer $PM_{2.5}$ aerosol (smaller particles) will be biased. This response can be theoretically predicted if one knows the particle size distribution and refractive index of the calibration aerosol as well as the test aerosol (Gorner et al. 1995). However, this is not possible in a field study where a large number of environments are sampled, and the aerosol characteristics will change with time.

Gravimetric Measurements

In addition to evaluating the performance of the pDR on a semi-continuous basis, comparisons to 24-hour time-integrated Federal Reference Methods (FRM) for $PM_{2.5}$ were also carried out. Over the course of the study when the pDRs were operating continuously, Teflon filters for mass measurements were deployed in both the Partisol sampler (FRM) and the back-up pDR filter holder for a total of twenty 24-hour periods (9AM to 9AM). The pDR filter sampling very accurately measures $PM_{2.5}$ mass relative to the FRM ($r^2 = 0.94$, slope = 1.01). Although not shown in a figure, the 24-hour averaged BAM concentrations are also in very good agreement with those measured with the Partisol, with an average BAM-to-Partisol ratio of 0.92 (± 0.13), and an r^2 equal to 0.77. These data are in agreement with the results of the Chung et al (2001) study and provide further corroboration to the integrity of the performance of the BAM. Considering the high degree of accuracy with respect to the FRM and other methods, this useful feature of the pDR allows a direct filter-based measurement of the total time-integrated mass of the exact same particles continuously monitored by the electronics of the pDR. The filter-based measurement might then be used to correct for the known biases of the electronic continuous pDR data. Also, when the humidity correction used above is applied to the continuous pDR on a fifteen minute basis, prior to 24-hour averaging, the correlation improves significantly to $r^2 = 0.56$. Table 1 also demonstrates how using the humidity correction improves the accuracy of the data. The geometric mean ratio between electronic and gravimetric data improves from 1.53 (± 0.28) to 1.06 (± 0.26) with the correction.

SUMMARY AND CONCLUSIONS

The field study of the active pDR monitors showed the instruments to be of sufficient precision and accuracy to be useful for personal exposure studies. The precision of the instruments is very high (2.1%) and significantly higher than the passive pDR configuration. Comparison to other proven continuous monitors revealed good agreement at lower relative humidities. Results at higher RH followed predictable theoretical and empirical trends that provide an accurate correction of pDR readings if RH is known. The response of the pDRs to particle size was also found to correspond to previously determined theoretical biases. The active flow configuration also allows collection of the sampled particles on a filter for subsequent gravimetric or chemical analysis. The particle mass collected on this back-up filter compared very well with Federal Reference Methods, and can be used as a secondary check on the electronically generated continuous data.

Although the current experiments were conducted on a laboratory bench and sampled outdoor aerosols, the authors feel that the results of this study will also apply to the performance of the pDR when deployed as a wearable monitor. The personal pumps and the pDRs are rugged and not effected by abrupt motion. The use of the $PM_{2.5}$ cyclone in conjunction with active flow

prevents larger dust particles, sometimes found indoors and in personal environments, from entering the chamber, settling on the optics, and biasing the results. In conjunction with a wearable humidity monitor and recorder, the active pDRs should prove useful in future exposure assessment and environmental health panel studies.

Fig. 1a. Correlation Between 15 Min Average pDR1 and pDR2 $PM_{2.5}$ Concentrations

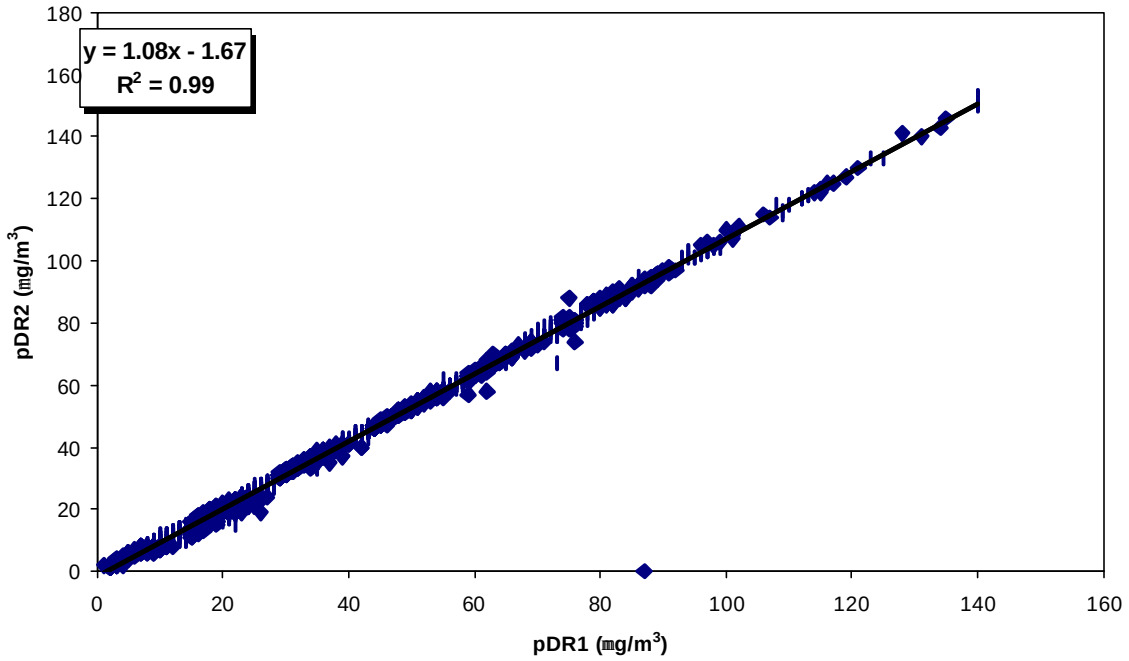

Fig. 1b. Correlation Between 15 Min Average pDR2 and pDR3 $PM_{2.5}$ Concentration

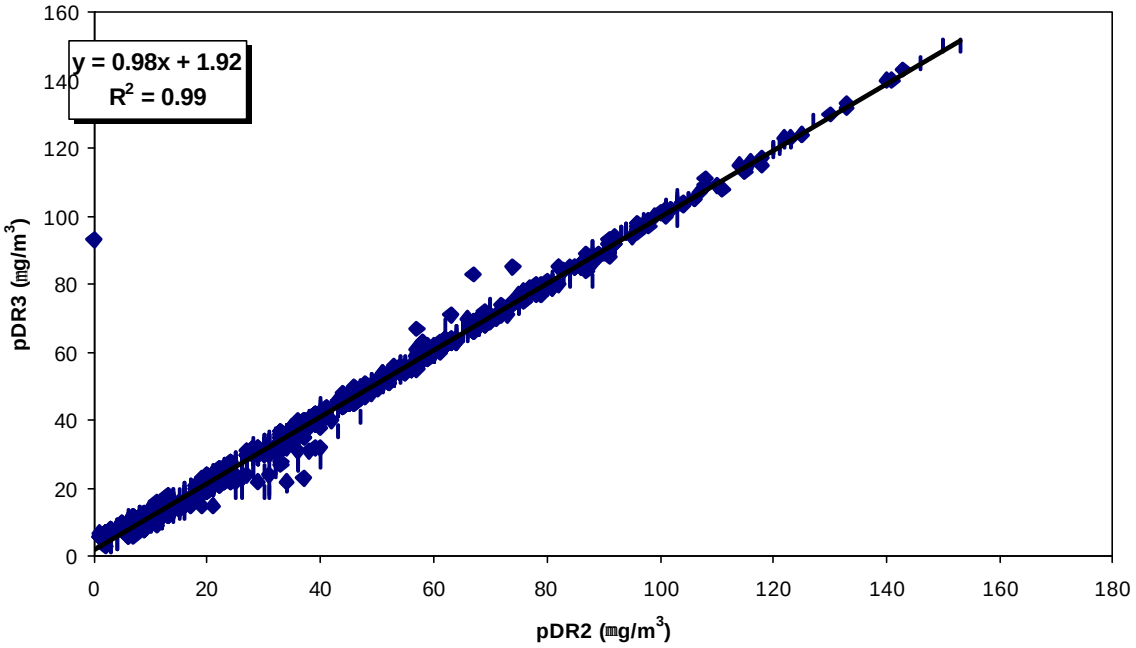

Fig. 2. Time Series of pDR1, pDR2, pDR3, and BAM $PM_{2.5}$ Concentrations (01/07/03-01/14/03)

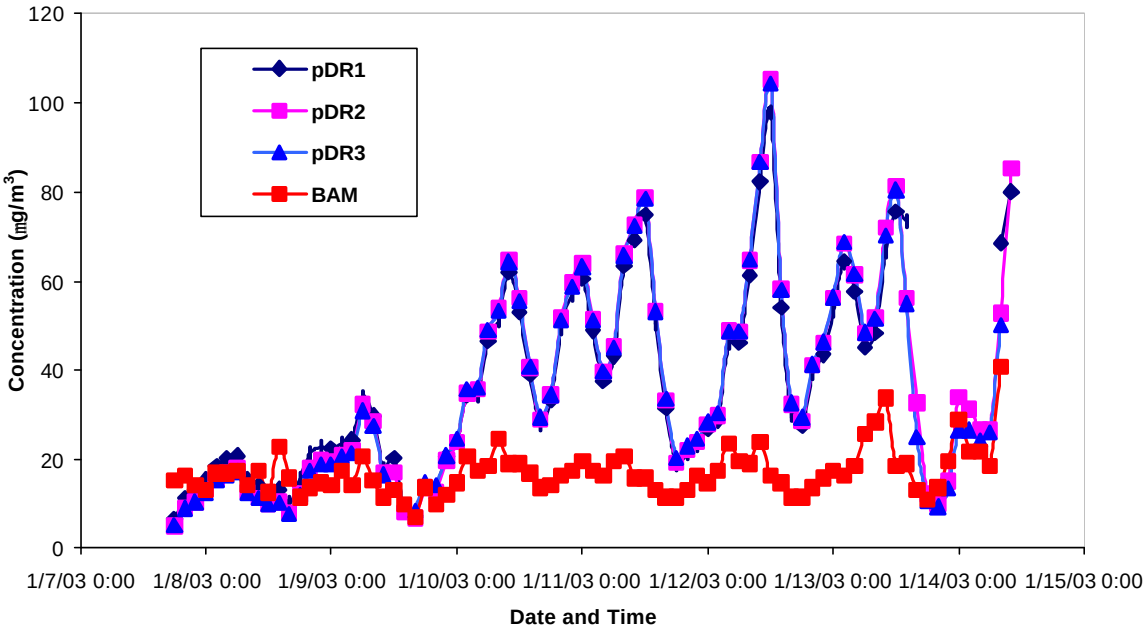

Fig.3. pDR to BAM Ratio as a function of Relative Humidity

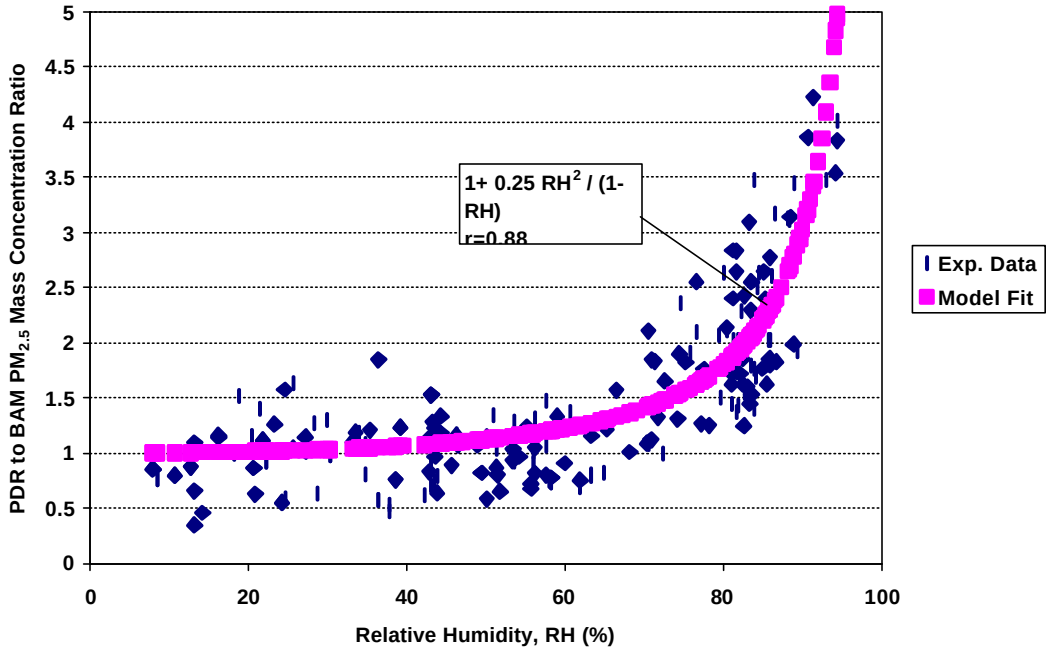

Fig. 4. $PM_{2.5}$ pDR and BAM Mass Concentrations for Relative Humidities Below 60%

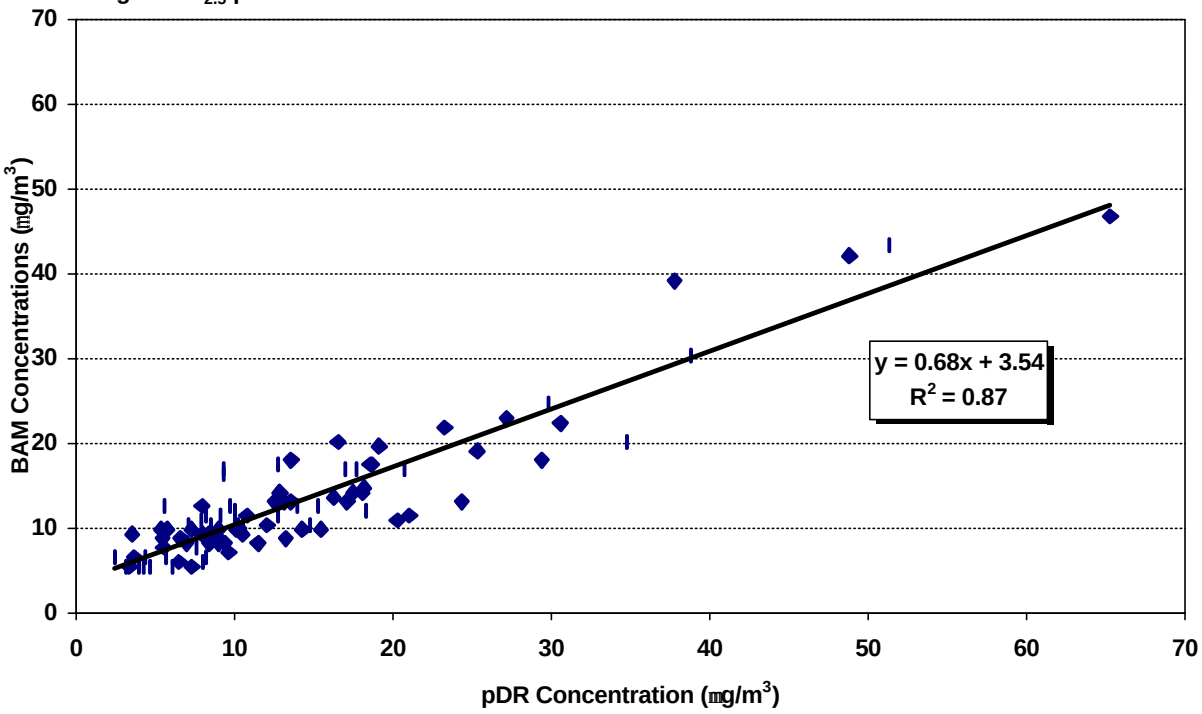

Fig. 5. Direct pDR to BAM $PM_{2.5}$ Concentration Ratio as a Function of Ambient Aerosol MMD

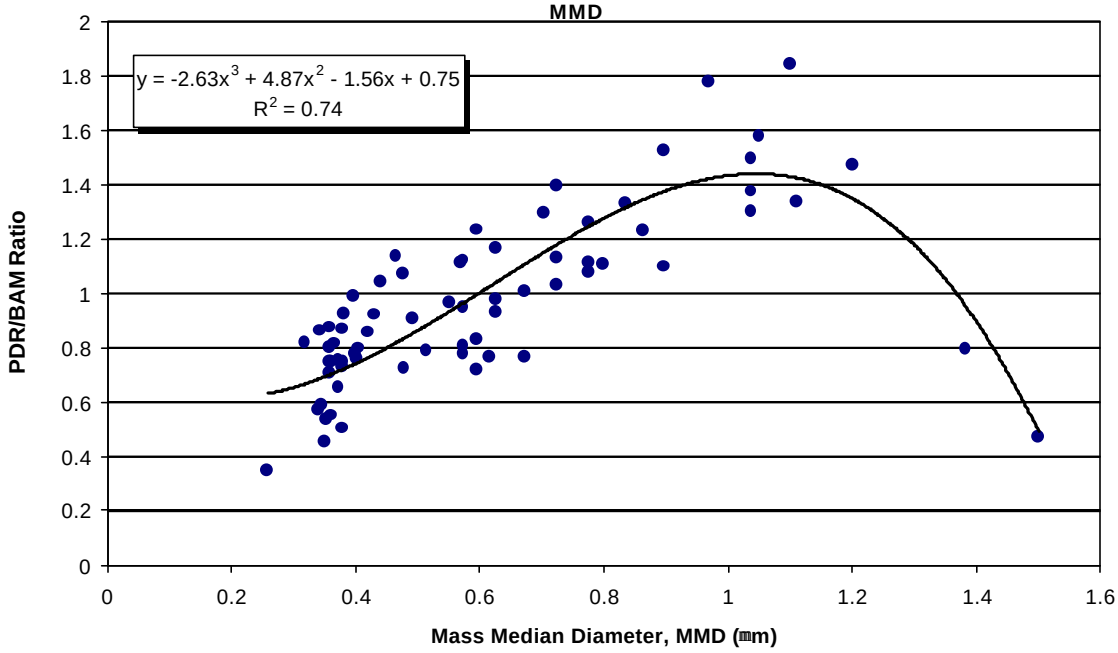

14. Development of a Near Continuous Monitor for Measurement of the Ultrafine PM Mass Concentration

ABSTRACT

Population exposures to ambient particulate matter (PM) have recently received considerable attention due to the association between ambient particle concentrations and mortality. Recent toxicological studies suggest that ultrafine PM (diameter < 150 nm) may be responsible for the observed health effects. However, even though ultrafine mass concentrations vary drastically over short time scales in the atmosphere, no monitor currently measures ultrafine PM mass continuously. The need for developing monitors for ultrafine particle concentration measurement in shorter time intervals is therefore of paramount importance to environmental health as it leads to substantial improvements in population exposure assessment to ambient ultrafine PM.

INTRODUCTION

This report presents the development of a modified Beta Attenuation Monitor (BAM, Model 1020, Met One instruments, Inc., OR) for near continuous (~2 hour) measurement of ultrafine PM mass concentrations. The BAM is preceded by a very low pressure drop, 0.15 μm cut point inertial impactor to remove all but ultrafine particles from the air sample. Sampling was conducted in the outdoor environment of Claremont- a receptor site of the Los Angeles Basin. The BAM is co-located with Microorifice Uniform Deposit Impactor (MOUDI™, MSP Corp. Minneapolis, MN; Marple et al.[15] 1991), a SMPS (TSI Model 3936) and an Aerodynamic Particle Sizer (APS, TSI Model 3320). The focus of the study is to document short-term variation in the ambient ultrafine particulate mass concentrations and to compare the BAM output with the time-integrated ultrafine mass concentration from the SMPS. The ratios of SMPS to BAM mass concentrations are studied for different time periods of the day. The correlations or lack thereof between ultrafine number concentrations from SMPS and mass concentrations from BAM are investigated for specific time periods of the day as well as for 24-hour averaged data. A similar exercise is carried out for ultrafine mass concentrations from BAM and the $PM_{2.5}$ mass concentrations provided by the SMPS-APS tandem.

METHODS

Instrumentation

The monitor for measuring ultrafine PM mass concentrations near continuously consists of a standard Beta Attenuation Monitor (BAM, Model 1020, Met One instruments, Inc., OR) preceded by a 0.15 μm cutpoint impactor. Ambient aerosols are drawn through the BAM at a sampling flow of 16.7 l min^{-1} via a vertical aluminum tube, 245 cm long and 3.3 cm in outer diameter. The lower end of the inlet tube is inserted directly into the top of BAM housing, the other end points horizontally upward above the roofline. The 0.15 μm cutpoint impactor is mounted on the upper end of the inlet tube. The modified BAM is operated in a 2-hour cycle.

The 0.15 μm cutpoint impactor is a single, rectangular (slit) jet geometry conventional impactor made of aluminum operating at a flow rate of 16.7 l min^{-1} and under a very low pressure drop (8 in H_2O or 0.019 kPa). Particles larger that the cutpoint are collected on a narrow strip of quartz filter substrate (Tissuquartz, Pall Gelman, Ann Arbor, MI). The impactor has a rectangular nozzle, 5 cm in length and 0.011 cm in width (W). The distance between the exit of the

acceleration nozzle plate and the impaction substrate is 0.0254 cm. The average jet velocity (U) corresponding to a flow of 16.7 l min^{-1} is about 50 m/s.

Sampling Location and Field Tests

The performance of BAM was evaluated in a field study conducted in July and early August of 2002 in Claremont, CA. The BAM was collocated with a MOUDI, a SMPS (Model 3936, TSI Inc), and APS (Model 3020, TSI Inc.). Direct comparisons were made between the time integrated averaged ultrafine PM concentrations measured by the BAM and those of the MOUDI corresponding to particles smaller than 0.15 µm in aerodynamic diameter. Sampling was conducted at Claremont, a downwind receptor site in the Los Angeles Basin, located approximately 45 miles east of downtown Los Angeles. The MOUDI operated at 30 l min^{-1} and sampled for 4-hour time intervals. 47-mm Teflon filters (PTFE, Gelman, 2 µm pore, Ann Arbor, MI) were used as impaction substrates, whereas particles smaller than 0.15 µm were collected on a 37-mm Teflon after-filter. Teflon filters of MOUDI™ were pre- and post-weighed using a Mettler Microbalance (MT5, Mettler-Toledo, Inc, Hightstown, NJ) after 24-hour equilibration under controlled humidity (35-40%) and temperature (22-24^{o}C) to determine particle mass concentrations.

RESULTS AND DISCUSSION

Laboratory Evaluation of the 150 nm Cutpoint Impactor

Results from the laboratory evaluation tests of the impactor are summarized in Figure 1. Particle collection efficiency data is plotted as a function of aerodynamic particle diameter. The results plotted in Figure 1 indicate that the experimentally determined 50% collection efficiency cutpoint is approximately 148 (± 10) nm in aerodynamic diameter. Particle collection efficiency increases rapidly with particle size to values exceeding 90% as particles become larger than about 250 nm in aerodynamic diameter. The ability to separate ultrafine PM from the rest of the aerosol under a very low pressure drop (0.019 kPa) is a particularly attractive feature of this impactor because it eliminates the need for using a high vacuum pump, thus makes it compatible with real-time (or continuous) instruments, such as the BAM, which typically operate using light, low powered pumps or blowers.

Ultrafine particle mass concentrations (integrated over 4-hour periods) measured by the BAM were compared with those obtained with MOUDI. Mass concentrations ranged from 1.50 ìg/m^3 to 8.98 ìg/m^3 for the BAM and 1.51 ìg/m^3 to 9.30 ìg/m^3 for the MOUDI, respectively. Inter-comparisons between BAM and MOUDI indicate an overall excellent agreement, with an average BAM to MOUDI concentration ratio of 0.92 (± 0.12). Figure 2 depicts the plot between ultrafine mass concentrations obtained with BAM and those obtained with MOUDI along with the linear regression line and the regression coefficient. As is evident from the figure, the BAM concentrations are highly correlated with those of MOUDI with $R^2 = 0.92$.

Comparisons between Ultrafine Mass Concentrations Obtained from BAM and SMPS

The average ratio of the SMPS-to-BAM ultrafine PM mass concentration, along with standard deviation, is plotted in Figure 3. The plotted mean ratios correspond to 2-hour data collected during July and early August of 2002. The SMPS-to-BAM concentration ratio is smaller than 1 for most of the time during the day indicating the mass concentration of the ultrafines estimated from

SMPS is always lower than those obtained from the BAM. The SMPS to BAM ratio resides between 0.4 – 0.5 from midnight to 9 a.m., then it increases rapidly to a range of 0.6-0.8 for up to about 4 p.m., and then again decreases to 0.4 - 0.5 during the late afternoon and evening hours. The maximum value of this ratio was observed at around noon and was about 0.77 (± 0.04). This distinctive diurnal profile is representative of all the days of the sampling period.

Figure 1: Laboratory Evaluation of the 150 nm Impactor

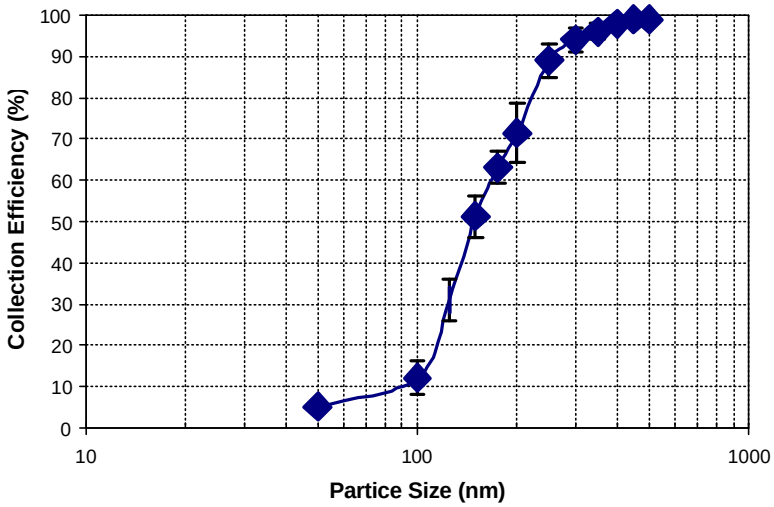

Figure 2: BAM vs. MOUDI Ultrafine PM concentration

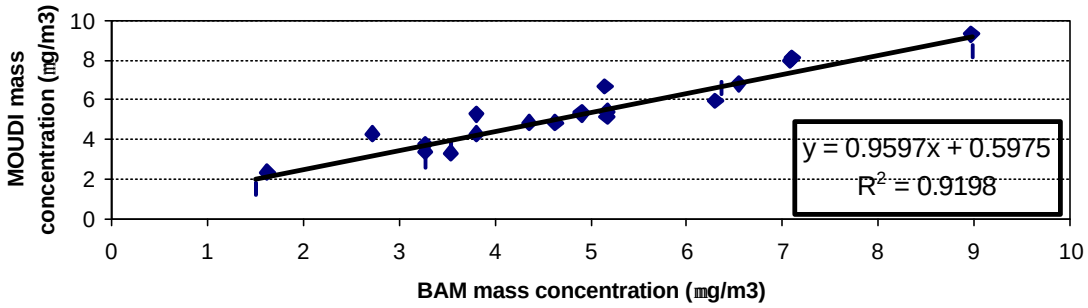

Figure 3: Diurnal Profile of SMPS to BAM Ratio of Mass Concenrations for the Ultrafines (07/07/2002-07/30/2002)

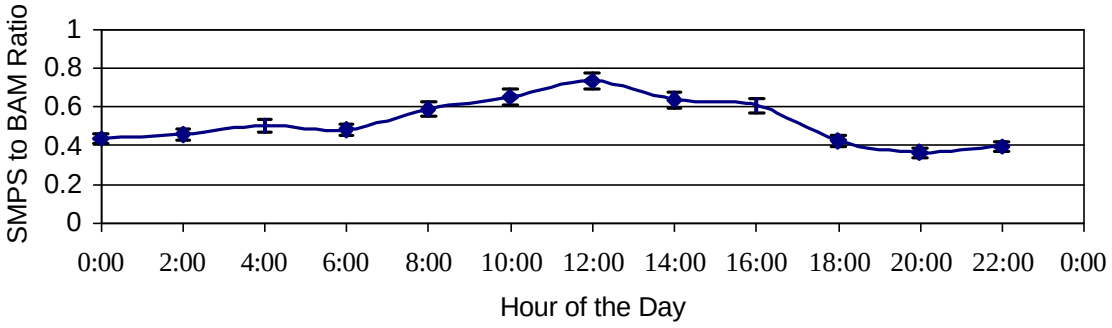

Field Evaluation of BAM

Correlations between Ultrafine Number, Mass and $PM_{2.5}$ Concentrations

As part of our investigation, we examined the relationship between the total particle number concentrations (determined by integrating the number-based concentrations of the SMPS), the ultrafine mass concentration (determined by the BAM) and the $PM_{2.5}$ mass concentrations measured by the SMPS. Based on data generated over the period of a month, no correlation seems to exist between the number and mass concentration of the ultrafine PM (Figure 4), with the R^2 value being only 0.06. Two time segments of the day were chosen to further investigate whether this correlation improves during the morning hours (6-9 a.m.) when the traffic rush is very high, and/or in the afternoon (2-6 p.m.) when photochemical reactions are the main PM sources in receptor areas of the Los Angeles basin, such as Claremont. A similar lack of correlation was observed between the $PM_{2.5}$ mass concentrations measured by the SMPS-APS and the ultrafine mass concentration monitored by the BAM. Further investigations of the correlation between the two concentrations at any specific period of the day, for example morning hours (6-9 a.m.) when traffic rush is at the maximum and for the evening hours (2-6 p.m.) when the photochemical reactions play the key role in particle formation, did not improve this relationship, with R^2 values of 0.001 and 0.13, respectively. These findings imply that $PM_{2.5}$ mass is a poor surrogate of the ultrafine component of $PM_{2.5}$, thus necessitates the need for developing continuous or near continuous monitoring system for ultrafine mass measurements if ultrafine particles prove to be responsible for health effects.

Figure 4:Correlation Between BAM (Mass Conc.) vs. SMPS (No. Conc.) for the Ultrafines from 07/03/02-08/05/02

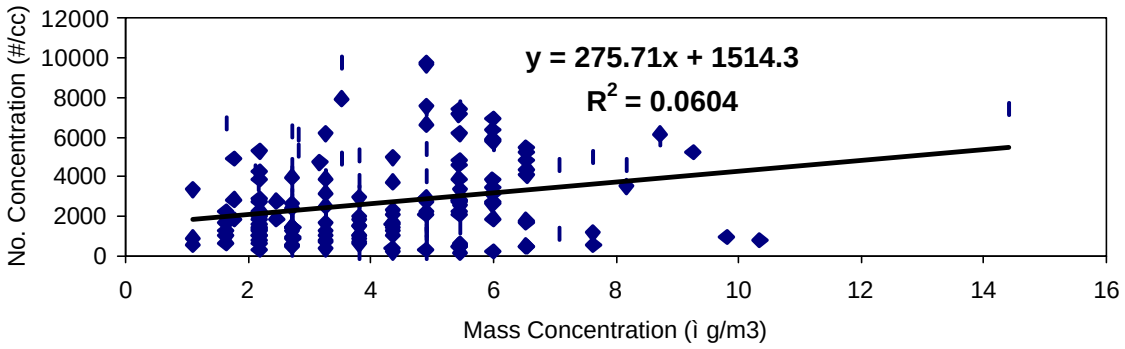

SUMMARY AND CONCLUSIONS

Findings from the field study ascertain that the present BAM setup can be used to measure reliably ultrafine mass concentrations, based on the excellent correlation between the BAM and the MOUDI (R^2=0.92) concentrations of particles smaller than 0.15 µm in aerodynamic diameter. Our study reveals that BAM is more accurate and efficient in measuring the ultrafine PM mass concentration compared to the SMPS. In virtually every sampling day of our study, the morning traffic peak in ultrafine mass concentrations measured by the modified BAM was undetected by the SMPS possibly due to the high content of fractal –like particles which tend to be classified in higher size ranges by the SMPS. The very poor correlation between the SMPS number concentrations and the BAM mass concentrations implies that further studies are necessary to determine whether the number or the mass of the ultrafines are best surrogates of their toxic effects. From the daily profile of the SMPS and BAM mass ratio, it can be inferred that the "effective" particle densities used for the calculation of the ultrafine PM mass from SMPS may vary over the course of the day. Finally the poor correlation between the $PM_{2.5}$ and the ultrafine mass concentrations demonstrate the need of the continuous monitoring requirement for the ultrafines for the effective assessment of the short-term variations in their mass concentration.

15. Quality Control of Semi-Continuous, Mobility Size-Fractionated Particle Number Concentration Data

This report summarizes the analysis that has been written up and submitted for publication to ***Atmospheric Environment***, as part of the Supersite special issues.

Authors: Rong Chun Yu, Hee Wen Teh, Peter A. Jaques, Constantinos Sioutas, and John R. Froines

Summary

Fine and ultrafine particles have been postulated to play an important role in the association between ambient particulate matters and adverse health effects. As part of the EPA Supersite Program, the Southern California Particle Center & Supersite (SCPCS) has conducted a series of monitoring campaigns that contribute to a better understanding of the sources, chemical composition and physical state of ambient aerosols. The Scanning Mobility Particle Sizer (SMPS) was deployed to semi-continuously measure mobility size-fractioned particle number concentrations. As part of the quality control efforts, we developed a two-stage graphic and statistical procedure to label and identify potentially discordant observations. The first stage considered the entire size-fractionated data by date-time as a whole to plot total concentration (TC) vs. coefficient of variation (CV), both in log scale. TC represents the magnitude of overall concentration for a size distribution; while CV represents the relative variability. This plot was used to partition all size distributions into four to five distinct regions. In each region, a generalized extreme studentized deviate (ESD) and a modified Z-score procedure were applied to identify potential discordant outliers. We have found that the majority of particle size distributions are concentrated within a 'normal' region, with TC ranging from 10^2 to 10^5 # cm^{-3} and CV varying between 20 to 200%. Size distributions that are contaminated with discordant outliers are displayed distinctly from the 'normal' region and form four to five clusters in the LogTC-LogCV plot. The pattern of clusters in the plot is consistent among the four sampling sites in this study, suggesting the robustness of this technique. The generalized ESD and modified Z score effectively identify discordant outliers and reveal that the pattern of clustering outliers are consistent within each distinct region. Based on our analysis, the main conclusions of our study are that:

1) Discordant outliers did occur in the particle size distributions generated by the SMPS system.
2) These outliers contaminated 'normal' particle size distributions in a manner that result in a clustering pattern found unique to the LogTC-LogCV plot. The pattern consists of more than four or five regions in which clusters of particle size distributions are typical.
3) Overall, for 4 separate monitoring sites, the rate of discordant outliers occurring in SMPS particle size distributions was approximately 0.021%.
4) The generalized ESD procedure performed well in identifying potential discordant outliers. However, it requires intensive computation.
5) The modified Z score procedure can be a useful tool for labeling potential outliers. However, the procedure is sensitive to the underlying statistical distribution of the SMPS size distribution. Furthermore, the procedure may generate false positive outliers, and fail to identify size distributions contaminated with discordant outliers.
6) The new approach is a useful quality control tool to identify potential discordant outliers in SMPS data.